Published for SISSA by Springer

Received: October 18, 2023
Revised: February 13, 2024
Accepted: March 2, 2024
Published: March 21, 2024

Search for dark matter particles in W^+W^- events with transverse momentum imbalance in proton-proton collisions at $\sqrt{s} = 13$ TeV

The CMS collaboration

E-mail: cms-publication-committee-chair@cern.ch

Abstract: A search for dark matter particles is performed using events with a pair of W bosons and large missing transverse momentum. Candidate events are selected by requiring one or two leptons (ℓ = electrons or muons). The analysis is based on proton-proton collision data collected at a center-of-mass energy of 13 TeV by the CMS experiment at the LHC and corresponding to an integrated luminosity of 138 fb^{-1}. No significant excess over the expected standard model background is observed in the $\ell\nu$qq and $2\ell2\nu$ final states of the W^+W^- boson pair. Limits are set on dark matter production in the context of a simplified dark Higgs model, with a dark Higgs boson mass above the W^+W^- mass threshold. The dark matter phase space is probed in the mass range 100–300 GeV, extending the scope of previous searches. Current exclusion limits are improved in the range of dark Higgs masses from 160 to 250 GeV, for a dark matter mass of 200 GeV.

Keywords: Beyond Standard Model, Dark Matter, Hadron-Hadron Scattering, Vector Boson Production

ArXiv ePrint: 2310.12229

https://doi.org/10.1007/JHEP03(2024)134

JHEP03(2024)134

Contents

1 Introduction

Astrophysical and cosmological observations [1–4] provide abundant evidence that dark matter (DM) exists. However, this evidence is based only on gravitational interactions, and whether DM has nongravitational interactions with standard model (SM) particles is still one of the major questions of fundamental physics. Many theories of new physics at the scale of electroweak (EW) symmetry breaking [5] propose viable candidates for DM and are able to accommodate the observed relic density of DM particles in the universe [6, 7]. Compelling contenders for DM are weakly interacting massive particles (WIMPs, denoted as χ) [8], which could be produced at high-energy colliders such as the Large Hadron Collider (LHC) at CERN. A favored DM signature in collider searches consists of one or more SM particles, X, that are produced and detected, recoiling against a pair of noninteracting DM particles that escape detection, resulting in missing transverse momentum ($p_{\mathrm{T}}^{\mathrm{miss}}$). Previous searches at the LHC took X to be a light quark producing a jet [9, 10], a heavy-flavor (bottom or top) quark [11, 12], a photon [13, 14], or a W, Z, or Higgs boson [10, 15–18].

An approach to probe DM at the LHC is based on a scenario in which the DM particle acquires mass through its interaction with a dark Higgs field [19]. The signal model used as a benchmark in this search posits a Majorana DM particle that transforms under a new

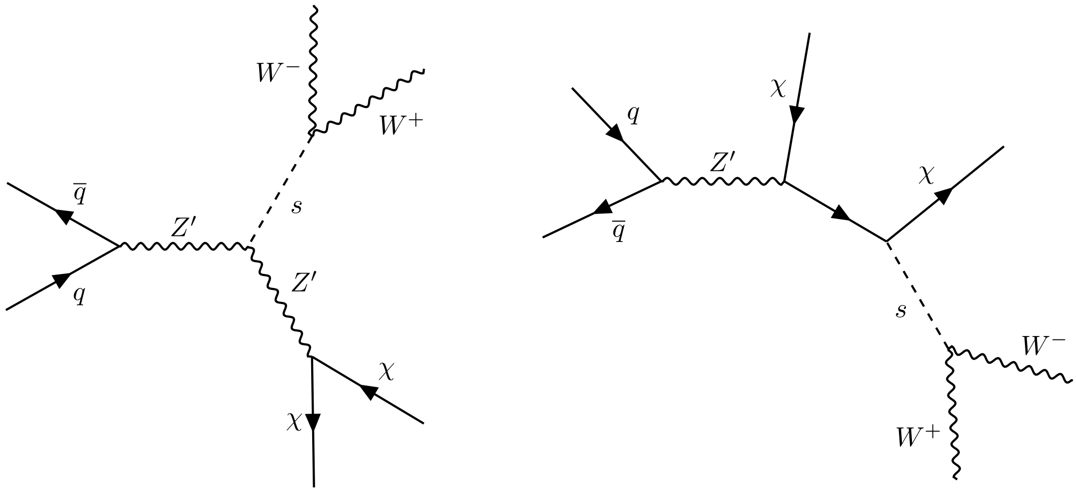

Figure 1. The dominant Born-level Feynman diagrams for the benchmark signal model considered in this paper: $\mathrm{q\bar{q}} \to \mathrm{Z}' \to \mathrm{s}\chi\chi$, and $\mathrm{s} \to \mathrm{W}^+\mathrm{W}^-$.

U(1) local gauge symmetry yielding an additional massive spin-1 vector boson Z' and a new physical dark Higgs boson s which is a singlet of the SM gauge groups. The Z' mediator could be responsible for establishing thermal equilibrium between the visible and the dark sector in the early universe and could provide the annihilation and creation processes that set the DM relic abundance via thermal freeze-out. Current results constrain the parameter space in which the DM particles can acquire their relic abundance from direct annihilation into SM final states [20]. This limitation can be significantly relaxed if the DM particle is not isolated as the lightest state in the dark sector. The dark Higgs boson can be lighter than the DM particle χ, in which case the observed relic abundance can readily be achieved through $\chi\chi \to \mathrm{ss}$ annihilation. Even if s is not strictly lighter than the DM candidate, the limitation can be evaded by the $\chi\chi \to \mathrm{sZ}'$ annihilation channel if m_s is low enough [21]. The dominant Born-level Feynman diagrams contributing to the s+$\chi\chi$ signature are shown in figure 1 and involve a Z' boson or χ intermediate state. The relevant model parameters are the DM mass m_χ, the Z' mass $m_{\mathrm{Z}'}$, the dark Higgs boson mass m_s, the Z' couplings to quarks (g_q) and to DM particles (g_χ), and the mixing angle (θ) between the SM and the dark Higgs bosons.

In this paper, a DM search is described using data recorded with the CMS detector at $\sqrt{s} = 13\,\mathrm{TeV}$ in 2016–2018, corresponding to an integrated luminosity of $138\,\mathrm{fb}^{-1}$. The X plus $p_\mathrm{T}^\mathrm{miss}$ signature is targeted, where X refers to the dark Higgs boson decaying to a $\mathrm{W}^+\mathrm{W}^-$ vector boson pair. For this paper, the signatures in which the W bosons both decay to charged leptons (ℓ = electrons or muons) and neutrinos ($2\ell2\nu$), or in which one decays to a charged lepton and a neutrino and the other decays to a pair of quarks ($\ell\nu$qq), are considered. For $m_\mathrm{s} > 160\,\mathrm{GeV}$, the $\mathrm{W}^+\mathrm{W}^-$ channel has the largest branching fraction [22]. This is the first search addressing such a dark Higgs model performed by the CMS Collaboration. Limits on this model have been published by the ATLAS Collaboration at $\sqrt{s} = 13\,\mathrm{TeV}$ using WW and ZZ channels, with the vector bosons decaying hadronically [23] or decaying to one lepton and jets [24].

This paper is organized as follows. A brief introduction to the CMS detector is given in section 2. The data and simulated event samples are described in section 3. The event reconstruction is detailed in section 4. The analysis strategy and the event selections are detailed in sections 5 and 6, respectively. Section 7 describes the background estimation and section 8 the systematic uncertainties. Finally, the results are presented in section 9, and the final summary is given in section 10. Tabulated results are provided in the HEPData record for this analysis [25].

2 The CMS detector

The central feature of the CMS apparatus is a superconducting solenoid of 6 m internal diameter, providing a magnetic field of 3.8 T. Within the solenoid volume are a silicon pixel and strip tracker, a lead tungsten crystal electromagnetic calorimeter (ECAL), and a brass and scintillator hadron calorimeter (HCAL), each composed of a barrel and two endcap sections. Forward calorimeters extend the pseudorapidity (η) coverage provided by the barrel and endcap detectors. Muons are detected in gas-ionization chambers embedded in the steel flux-return yoke outside the solenoid. The first level of the CMS trigger system [26], composed of custom hardware processors, is designed to select the most interesting events within a time interval of less than 4 μs, using information from the calorimeters and muon detectors, with an output rate of up to 100 kHz. The high-level trigger processor farm further reduces the event rate to about 1 kHz before data storage. A more detailed description of the CMS detector, together with a definition of the coordinate system used and the relevant kinematic variables, can be found in ref. [27].

3 Data and simulated samples

The proton-proton (pp) collision data used in this search were collected at $\sqrt{s} = 13$ TeV during 2016, 2017, and 2018, with integrated luminosities of 36.3, 41.5, and 59.8 fb^{-1}, respectively [28–30]. The average number of multiple pp interactions per bunch crossing (pileup) is approximately 23 for the 2016 data, and 32 for the 2017–2018 data.

Events are stored if they satisfy the selection criteria of online triggers requiring one or two leptons with a minimum transverse momentum (p_{T}) requirement. The lowest p_{T} thresholds for the double-lepton triggers are 23 GeV for the leading lepton (ℓ_{max}) and 12 GeV for the next-to-leading lepton (ℓ_{min}). The single-lepton triggers in the 2016 data set have p_{T} thresholds of 25 GeV for $|\eta| < 2.1$ and 27 GeV for $2.1 < |\eta| < 2.5$ for electrons, and of 24 GeV for muons. In the 2017 data set, the thresholds are increased to 35 for electrons and 27 GeV for muons, while in the 2018 data set they are reduced to 32 and 24 GeV, respectively. The trigger efficiency is measured using Z+jets events and is larger than 90% for both electrons and muons over the given η range.

Monte Carlo (MC) simulated events are used for modeling both signal and background processes. Event samples for 2016, 2017, and 2018 data sets are simulated separately to account for the differences in the detector and pileup conditions. Different parton distribution functions (PDFs) and underlying event (UE) tunes are used for the different simulated data sets. In all simulations, the PYTHIA [31] 8.226 (8.230) library is used for parton showering,

JHEP03(2024)134

hadronization, and the UE simulation, using the CUETP8M1 [32] (CP5 [33]) tune for 2016 (2017–2018). Similarly, the NNPDF 3.0 [34, 35] PDF set is used for the 2016 data set, while the NNPDF 3.1 [36] set is used for the 2017–2018 data sets.

Signal samples are generated at leading order (LO) in perturbative quantum chromodynamics (QCD) using the MadGraph5_aMC@NLO v2.6.5 generator [37], applying the PYTHIA CP5 tune for all three years. A scan in the (m_s, $m_{Z'}$, m_χ) parameter space is performed on 672 points between $160 < m_s < 400$ GeV, $200 < m_{Z'} < 2500$ GeV, and $100 < m_\chi < 300$ GeV, while the other model parameters are fixed to $g_\chi = 1.00$, $g_q = 0.25$, and $\sin\theta = 0.01$. The Z′ and s boson widths vary slightly depending on the selected parameters and are confirmed to be below 1% of their respective masses. The chosen values for these parameters correspond to those recommended as a benchmark in the LHC Dark Matter Working Group (LHC DM WG) [19, 38].

Continuum W^+W^- production background via $q\bar{q}$ annihilation is generated with POWHEG v2 at next-to-LO (NLO) precision [39], while gg → WW events are generated at LO using MCFM v7.0 [40, 41]. The simulated $q\bar{q}$ → WW events are reweighted to match the p_T distribution of the WW-system (p_T^{WW}) from the p_T-resummed calculation at next-to-NLO plus next-to-next-to-leading logarithmic precision [42, 43], and to account for the higher-order EW effects [44]. The LO gg → WW cross section, obtained from MCFM, is scaled to next-to-NLO precision via a K factor of 1.4 [45]. The different Higgs boson production modes are generated with POWHEG v2 [46–52] and the $H \to W^+W^-$ decay with JHUGen [53]. Single top quark, $t\bar{t}$, WZ, and $W\gamma^*$ background processes are generated at NLO with POWHEG v2. To further improve the modelling of $t\bar{t}$ production, the simulated samples are reweighted based on the p_T of each top quark [54]. Production of a single W boson in association with jets is simulated at LO using MadGraph5_aMC@NLO v2.2.2 and v2.6.5 for 2016 and 2017–2018 samples respectively. The description of the W+jets process is improved by scaling the events to kinematic distributions computed at NLO EW precision [55]. The QCD K factors are derived from NLO samples as a function of the generated p_T of the W boson. Variations of up to 12% of the simulated event yields due to different generator versions and settings across the sample years are compensated for with an additional K factor depending on the reconstructed dijet mass, and treated as uncertainties. Drell-Yan (DY) production of Z/γ^*, and other multiboson processes, such as $W\gamma$, ZZ, and VVV (V = W or Z), are generated at NLO using MadGraph5_aMC@NLO. All samples are normalized to the latest available theoretical cross sections with at least NLO precision [40, 56]. For all the processes, the detector response is simulated using the Geant4 toolkit [57].

4 Event reconstruction

The primary vertex (PV) is taken to be the vertex corresponding to the hardest scattering in the event, evaluated using tracking information alone, as described in section 9.4.1 of ref. [58].

A particle-flow (PF) algorithm [59] aims to reconstruct and identify individual particles in an event with an optimized combination of information from the various elements of the CMS detector. The energy of photons is obtained from the ECAL measurement. The energy of charged hadrons is determined from a combination of their momentum measured in the tracker and the matching ECAL and HCAL energy deposits, corrected for the response

JHEP03(2024)134

function of the calorimeters to hadronic showers. The energy of neutral hadrons is obtained from the corresponding corrected ECAL and HCAL energies.

Electrons are reconstructed using information from the pixel detector, the silicon strip tracker, and the ECAL in the interval $|\eta| < 2.5$. The track is required to be consistent with originating from the PV. The electron momentum is estimated by combining the energy measurement in the ECAL, the momentum measurement in the tracker, and the energy sum of all bremsstrahlung photons spatially compatible with the electron track. The efficiency to reconstruct and identify electrons ranges between 60–80% depending on the electron p_{T} and η. The momentum resolution for electrons with $p_{\mathrm{T}} \approx 45\,\mathrm{GeV}$, measured in $\mathrm{Z} \to \mathrm{ee}$ decays, ranges from 1.7–4.5%, depending on the η region and on the bremsstrahlung energy emitted by the electron as it traverses the material in front of the ECAL [60].

Muons are reconstructed in the interval $|\eta| < 2.4$ using the information from the muon chambers and the silicon tracker, and they are required to be consistent with the reconstructed PV. The efficiency to reconstruct and identify muons is greater than 96%. The relative p_{T} resolution for muons with p_{T} up to 100 GeV is 1% in the barrel and 3% in the endcaps [61, 62].

Both electrons and muons are required to be isolated. In the case of an electron, the scalar p_{T} sum of other PF candidates within a cone of size $\Delta R = \sqrt{(\Delta\eta)^2 + (\Delta\phi)^2} < 0.3$ (where ϕ is the azimuthal angle in radians) around its direction is required to be less than 6% of the electron p_{T}. Only those PF candidates associated with the PV are included in the isolation sum. In case of a muon, the p_{T} sum is evaluated for PF candidates in a cone $\Delta R < 0.4$ and is required to be less than 15% of the muon p_{T}.

Jets in each event are clustered from the neutral and charged PF candidates associated with the PV, using the anti-k_{T} algorithm [63, 64] with a distance parameter of $R = 0.4$. The expected average contribution from pileup is subtracted from the reconstructed jet energy [59]. Additional selection criteria are applied to each jet with $p_{\mathrm{T}} > 15\,\mathrm{GeV}$ and $|\eta| < 4.7$ to remove those potentially dominated by anomalous contributions from various subdetector components or reconstruction failures [65]. For the 2017 data sets, jets in the range $2.5 < |\eta| < 3.0$ are excluded to eliminate spurious jets caused by the detector noise. The jet energy resolution typically amounts to 15% at 10 GeV, 8% at 100 GeV, and 4% at 1 TeV [66].

The identification of jets containing hadrons with bottom (b) quarks is referred to as b tagging. For each reconstructed jet, a b tagging score is calculated through a multivariate analysis of jet properties using a fully-connected deep neural network based algorithm, DeepCSV [67]. Jets are considered b tagged if the DeepCSV b tag output score is above a threshold set to achieve $\approx 80\%$ efficiency for b quark jets in $\mathrm{t\bar{t}}$ events. For this threshold, the probability of misidentifying a jet as b quark jet in $\mathrm{t\bar{t}}$ events is $\approx 11\%$ for light-flavor or gluon jets and $\approx 41\%$ for charm quark jets.

The vector ($\vec{p}_{\mathrm{T}}^{\,\mathrm{miss}}$), with magnitude $p_{\mathrm{T}}^{\mathrm{miss}}$, is defined as the negative vector p_{T} sum of all the PF candidates in an event [68], weighted by their estimated probability to originate from the primary interaction vertex. The pileup-per-particle identification algorithm [69] is employed to calculate this probability. Energy scale corrections to the reconstructed jets are taken into account in this computation.

5 Analysis strategy

This analysis exploits the dependence of the kinematic properties of the final-state objects (the decay products of the W^+W^- boson pair and a substantial amount of p_T^{miss} from DM) on the three parameters m_s, $m_{Z'}$ and m_χ, which enables the separation of signal events from the main background events.

For the $2\ell 2\nu$ channel, the observable chosen to test the dark Higgs model is the transverse mass of the ℓ_{min} plus p_T^{miss} system, the distribution of which is more sensitive to the predicted dark Higgs signal than other observables based on the kinematic properties of the lepton or p_T^{miss}. This transverse mass is defined as:

$$m_T^{\ell_{min},p_T^{miss}} = \sqrt{2p_T^{\ell_{min}} p_T^{miss} \left[1 - \cos\Delta\phi(\vec{p}_T^{\,\ell_{min}}, \vec{p}_T^{\,miss})\right]}, \tag{5.1}$$

where $p_T^{\ell_{min}}$ is the magnitude of the p_T vector of the ℓ_{min} candidate, and $\Delta\phi(\vec{p}_T^{\,\ell_{min}}, \vec{p}_T^{\,miss})$ is the azimuthal angle between $\vec{p}_T^{\,\ell_{min}}$, and the $\vec{p}_T^{\,miss}$. The signal is extracted from a two-dimensional profiled maximum likelihood fit to the invariant mass of the dilepton system, $m_{\ell\ell}$ and the $m_T^{\ell_{min},p_T^{miss}}$ observable with a signal-plus-background hypothesis using the RooStats Project tools [70]. The asymptotic approximation of the profile likelihood ratio [71] is used as a test statistic.

For the $\ell\nu$qq channel, because of the relatively low expected cross section of the signal processes and the large irreducible W+jets background, the variables that show most promising separation of signal and background are combined in a boosted decision tree (BDT) to produce a single discriminator. From the initial set of 23 candidate variables, a subset of 13 variables is selected by comparing intermediate BDTs in terms of background rejection and signal selection efficiency. An overview of all selected variables and their descriptions is given in table 1. The resulting discriminator returns values between -1, the background-like extreme, and 1, the most signal-like. It has been cross-checked that events with values at the lower end are predominantly background, while signal events accumulate at higher values. The final analysis results are obtained from a fit to the binned BDT discriminator distribution, as described in section 9.

6 Event selection

6.1 The $2\ell 2\nu$ channel

The main feature of the $s \to W^+W^-$ decay in the $2\ell 2\nu$ channel is the presence of two oppositely charged and isolated leptons with relatively large p_T, recoiling against $\vec{p}_T^{\,miss}$. The analysis imposes a set of requirements on kinematic and topological quantities aimed at defining a phase space enriched in $s \to W^+W^-$ events.

In addition to the requirement of opposite charge, the leptons are required to be well-identified, isolated, and have different flavors. In order to reduce the contamination from the DY process, final states with same-flavor leptons are excluded in this analysis. The $p_T^{\ell_{max}}$ is required to be greater than 25 GeV and the $p_T^{\ell_{min}}$ has to be greater than 20 GeV, to ensure a good reconstruction and identification efficiency. The dilepton system is required

Variable	Definition
p_T^{jj}	p_T of the vectorial sum of the W candidate jets
$p_T^{\ell jj}$	p_T of the vectorial sum of the visible particles
p_T^{miss}	Magnitude of the missing transverse momentum vector
$\Delta\eta_{\ell,jj}$ and $\Delta\phi_{\ell,jj}$	$\Delta\eta$ and $\Delta\phi$ between the lepton and the dijet system
$\Delta\eta_{j,j}$ and $\Delta\phi_{j,j}$	$\Delta\eta$ and $\Delta\phi$ between the W candidate jets
$\lvert\eta_\ell\rvert$	The absolute value of the lepton pseudorapidity
$\Delta\phi_{\ell,\vec{p}_T^{miss}}$	$\Delta\phi$ between the lepton and $\vec{p}_T^{miss}$
$\Delta\phi_{\ell jj,\vec{p}_T^{miss}}$	$\Delta\phi$ between the vectorial sum of the visible particles and $\vec{p}_T^{miss}$
$\min(p_T^\ell, p_T^{j_2})/p_T^{miss}$	Minimum of the lepton p_T and the next-to-leading W candidate jet p_T, divided by p_T^{miss}
$\max(p_T^\ell, p_T^{j_1})/p_T^{miss}$	Maximum of the lepton p_T and the leading W candidate jet p_T, divided by p_T^{miss}
$\max(p_T^\ell, p_T^{j_1})/m_{\ell jj p_T^{miss}}$	Maximum of the lepton p_T and the leading W candidate jet p_T, divided by the invariant mass of the system of all visible particles and $\vec{p}_T^{miss}$, which is taken to be massless

Table 1. Summary of all selected variables considered in the BDT for the $\ell\nu$qq channel.

to have a minimum invariant mass $m_{\ell\ell}$ of 20 GeV in order to eliminate low-mass DY. The transverse momentum of the lepton pair $p_T^{\ell\ell}$must be greater than 30 GeV, to reduce background contributions from leptons that do not originate from the PV (nonprompt leptons). To minimize the impact of multilepton contributions from WZ and ZZ backgrounds, events that include a third lepton, which is subjected to less strict selection criteria compared to the lepton identification used for the two high-p_T leptons, are rejected if its p_T is larger than 10 GeV. Events with one or more b-tagged jets with transverse momentum $p_T^b > 20$ GeV are rejected. This selection reduces the background from top quark production by ≈ 86% while losing less than 10% of signal events.

To further suppress DY background, a minimum value of the transverse mass of the dilepton system plus p_T^{miss} is required, $m_T^{\ell\ell,p_T^{miss}} > 50$ GeV, and a selection on the quantity $p_T^{miss,proj}$ [72] is introduced. This quantity is defined as the component of $\vec{p}_T^{miss}$ in the direction of the nearest lepton if the lepton is situated within the azimuthal angular cone of $\pm\pi/2$ from the $\vec{p}_T^{miss}$ direction, or the p_T^{miss} otherwise. A selection using this variable efficiently rejects $Z/\gamma^* \to \ell\ell$ background events in which the $\vec{p}_T^{miss}$ is preferentially aligned with leptons. Since the p_T^{miss} resolution is degraded by pileup, a quantity is defined as the smaller of the two $p_T^{miss,proj}$ values: one based on all the PF candidates in the event ($p_T^{miss,PF\ proj}$), and the other one based only on the reconstructed tracks originating from the PV ($p_T^{miss,track\ proj}$). This quantity is required to be larger than 20 GeV. These selection requirements remove ≈ 95% of the DY background and less than 5% of the signal.

A summary of the event selection is shown in table 2, and the $m_T^{\ell_{min},p_T^{miss}}$ distribution for signal and leading backgrounds is shown in figure 2.

Quantity	Selection
Number of leptons	2
Lepton flavors	eμ
Lepton charges	Opposite
Additional leptons	0
$p_T^{\ell_{max}}$	>25 GeV
$p_T^{\ell_{min}}$	>20 GeV
$m_{\ell\ell}$	>20 GeV
$p_T^{\ell\ell}$	>30 GeV
p_T^{miss}	>20 GeV
$\min(p_T^{miss,PF\ proj}, p_T^{miss,track\ proj})$	>20 GeV
$m_T^{\ell\ell,p_T^{miss}}$	>50 GeV
$\Delta R_{\ell\ell}$	<2.5
Number of b-tagged jets	0

Table 2. Summary of the event selection criteria in the $2\ell 2\nu$ channel.

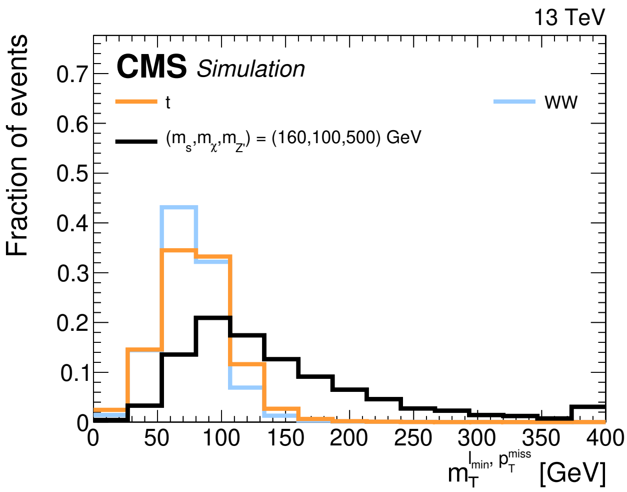

Figure 2. Normalized $m_T^{\ell_{min},p_T^{miss}}$ distribution in the $2\ell 2\nu$ channel for a signal with $m_s = 160$ GeV, $m_\chi = 100$ GeV, $m_{Z'} = 500$ GeV (black), after the event selection criteria are applied. Predictions for the two main backgrounds of the analysis, WW and t production, are shown as blue and yellow solid lines respectively. The last bin includes the overflow. The t production sample consists of approximately 79% t quark pair production and 21% single t processes.

To account for the dependence of the kinematic properties of the final-state objects on the mass of the dark Higgs boson, the events that pass the event selection described above are categorized into three signal regions (SRs). The split is based on a proxy of the Lorentz boost of the dark Higgs boson recoiling against the DM system by considering the distance between the two leptons in the (η,ϕ) plane, $\Delta R_{\ell\ell}$. An optimized division is achieved in SR1: $\Delta R_{\ell\ell} < 1.0$ (high-boost); SR2: $1.0 < \Delta R_{\ell\ell} < 1.5$ (medium-boost);

JHEP03(2024)134

Year	Electron p_{T}	Muon p_{T}
2016	>25 GeV	>24 GeV
2017	>35 GeV	>27 GeV
2018	>32 GeV	>24 GeV

Table 3. Selection criteria for the leptons for 2016–2018 data in the $\ell\nu$qq channel. The p_{T} thresholds are chosen to be equal to the corresponding single-lepton trigger threshold.

and SR3: $1.5 < \Delta R_{\ell\ell} < 2.5$ (low-boost) by carefully balancing the signal efficiency and background rejection. Approximately 33% of the background is rejected by selecting events with $\Delta R_{\ell\ell} < 2.5$, with a negligible effect on the signal.

6.2 The $\ell\nu$qq channel

The main feature in the $\ell\nu$qq channel of the $\mathrm{s} \to \mathrm{W^+W^-}$ decay is the presence of one well-reconstructed and isolated lepton and at least two jets recoiling against $\vec{p}_{\mathrm{T}}^{\,\mathrm{miss}}$. Different lepton preselections are used for each data set to comply with the varying trigger selection thresholds; they are listed in table 3. Events containing a second loosely-defined lepton with $p_{\mathrm{T}} > 10\,\mathrm{GeV}$ are vetoed.

When more than two jets are available, the pair having an invariant mass closest to the W boson mass are selected as W candidate jets. Both W candidate jets are required to be within the tracker acceptance region ($|\eta| < 2.4$) to avoid the high multiplicity of background particles produced in the high-$|\eta|$ regions. Events with jets that do not originate from a W boson are suppressed by requiring $65 < m_{\mathrm{jj}} < 105\,\mathrm{GeV}$. The contribution of top quark background events to the SR is further reduced by removing events with at least one b-tagged jet, with $p_{\mathrm{T}} > 20\,\mathrm{GeV}$, that is not tagged as a W candidate jet.

All background events can be further suppressed by comparing the kinematic variables of the visible particles and $p_{\mathrm{T}}^{\mathrm{miss}}$. The presence of DM candidates in an event results in a large $p_{\mathrm{T}}^{\mathrm{miss}}$ well separated from visible particles as compared to SM processes. Thus, we impose the requirements $p_{\mathrm{T}}^{\mathrm{miss}} > 60\,\mathrm{GeV}$ and $m_{\mathrm{T}}^{\ell,p_{\mathrm{T}}^{\mathrm{miss}}} > 80\,\mathrm{GeV}$ where

$$m_{\mathrm{T}}^{\ell,p_{\mathrm{T}}^{\mathrm{miss}}} = \sqrt{2\,p_{\mathrm{T}}^{\ell} p_{\mathrm{T}}^{\mathrm{miss}} [1 - \cos(\Delta\phi_{\ell,\vec{p}_{\mathrm{T}}^{\,\mathrm{miss}}})]}. \tag{6.1}$$

These two kinematic requirements are especially effective in decreasing the amount of nonprompt-lepton and DY background. Another feature of the signal events is that the visible particles tend to cluster azimuthally in the direction opposite to $\vec{p}_{\mathrm{T}}^{\,\mathrm{miss}}$. For these reasons, $\Delta R_{\ell,\mathrm{jj}}$ is required to be smaller than 3.0, $\Delta\phi_{\ell,\mathrm{jj}}$ is required to be below 1.8, $\Delta\phi_{\ell\mathrm{jj},\vec{p}_{\mathrm{T}}^{\,\mathrm{miss}}}$ must be above 2.0, and $p_{\mathrm{T}}^{\ell\mathrm{jj}}$ must be above 60 GeV.

These additional topological requirements remove $\approx 97\%$ of the background ($\approx 97\%$ for W+jets, $\approx 94\%$ for t production, and $\approx 99\%$ for nonprompt-lepton events) while keeping between 60–80% of signal events. An optimal differentiation of signal and background events is accomplished using a BDT for which these variables are inputs. A summary of the event selection criteria for the $\ell\nu$qq channel is shown in table 4.

JHEP03(2024)134

Quantity	Selection
Number of leptons	1
Additional leptons	0
Number of jets	≥2
Non-W-candidate b-tagged jets	0
m_{jj}	>65 GeV, <105 GeV
$p_{\mathrm{T}}^{\mathrm{miss}}$	>60 GeV
$p_{\mathrm{T}}^{\ell\mathrm{jj}}$	>60 GeV
$m_{\mathrm{T}}^{\ell,p_{\mathrm{T}}^{\mathrm{miss}}}$	>80 GeV
$\Delta R_{\ell,\mathrm{jj}}$	<3.0
$\Delta\phi_{\ell,\mathrm{jj}}$	<1.8
$\Delta\phi_{\ell\mathrm{jj},\vec{p}_{\mathrm{T}}^{\mathrm{miss}}}$	>2.0

Table 4. Summary of the event selection criteria for the $\ell\nu$qq channel.

7 Background estimation

All background processes, except those with nonprompt leptons, are modeled using MC simulations. The nonprompt-lepton background is estimated from data by examining events selected with less stringent lepton selection criteria. These loose leptons have a relative high probability to originate from jets that have been incorrectly categorised. By measuring the rate of these misidentified loose leptons erroneously passing the SR criteria and the efficiency of correctly reconstructing and identifying a lepton, the nonprompt contribution to the SR can be estimated. Details of this method are given in ref. [72]. The validity of this background estimation is checked in a validation region. For the $2\ell2\nu$ selection, this region is defined by requiring two same-sign leptons while keeping the other selection criteria the same as those listed in table 2. In the $\ell\nu$qq case, the requirements $p_{\mathrm{T}}^{\mathrm{miss}} < 30\,\mathrm{GeV}$ and $m_{\mathrm{T}}^{\ell,p_{\mathrm{T}}^{\mathrm{miss}}} < 30\,\mathrm{GeV}$ replace the corresponding selections of table 4, exploiting the fact that events with a nonprompt lepton do not necessarily have a neutrino, resulting in a relatively small $p_{\mathrm{T}}^{\mathrm{miss}}$.

The normalizations of the most important background processes are determined from the observed data in certain control regions (CRs). The main backgrounds consist of the $\mathrm{W^+W^-}$ and DY processes for the $2\ell2\nu$ channel, W+jets events for the $\ell\nu$qq channel, and t production for both. One CR is defined for each process:

- The t production CR is defined by requiring the presence of at least one b-tagged jet, thereby inverting the b-veto.
- In the $2\ell2\nu$ channel, the $\mathrm{W^+W^-}$ CR is defined by inverting the $\Delta R_{\ell\ell}$ selection, i.e., $\Delta R_{\ell\ell} > 2.5$.
- In the $2\ell2\nu$ channel, the DY CR is defined by inverting the $m_{\mathrm{T}}^{\ell\ell,p_{\mathrm{T}}^{\mathrm{miss}}}$ requirement, i.e., $m_{\mathrm{T}}^{\ell\ell,p_{\mathrm{T}}^{\mathrm{miss}}} < 50\,\mathrm{GeV}$.

JHEP03(2024)134

- In the $\ell\nu$qq channel, the W+jets CR is defined by inverting the m_{jj} selection, i.e., $m_{jj} < 65$ or > 105 GeV.

The event yields in these four CRs are fitted simultaneously with the SRs, letting the W^+W^-, DY, W+jets and t production normalizations float freely in all CRs and SRs. A possible signal contribution in the CRs is also taken into account.

8 Systematic uncertainties

Experimental and theoretical sources of systematic uncertainty are described in this section. Effects from experimental uncertainties are studied by scaling and/or smearing the reconstructed objects in simulation and propagating the effect to the kinematic variables used in the analysis.

There are several sources of experimental systematic uncertainties, including the lepton reconstruction and identification efficiencies, the lepton momentum scales, the jet energy scale and resolution, the b tagging efficiency for b quark jets, the mistag rate for light-flavor quark and gluon jets, the modeling of p_T^{miss} and of pileup in the simulation, the background contributions, and the integrated luminosity. All experimental sources are treated as uncertainties that either change the shapes of the distributions or scale the normalizations of the individual signal and background processes. In the simultaneous fit, the different sources of uncertainty are each represented by single independent nuisance parameters. When combining the uncertainties across processes and data sets, they are treated as correlated or uncorrelated as appropriate.

Lepton efficiency uncertainties are evaluated as functions of the lepton p_T and η, using the tag-and-probe method. The impact of the trigger efficiency uncertainty is less than 1 (2)% overall in the $2\ell2\nu$ ($\ell\nu$qq) analysis, while the uncertainties in the reconstruction and identification efficiency cause shape and normalization changes of $\approx 1.0\%$ ($\approx 1.0\%$) for electrons and ≈ 2.0 (≈ 0.5)% for muons. Changes in lepton momentum scale are at the level of 0.2 (0.4)% for muons and ≈ 0.6–1.0 (≈ 0.1–0.8)% for electrons. Those uncertainties are propagated to p_T^{miss} resulting in a total variation of 1–10%. For the changes in the jet energy scale, the impact on the normalization is $\approx$1% for the $2\ell2\nu$ search, while for the $\ell\nu$qq case, the impact can be as large as 10%.

Experimental uncertainties in the estimation of the nonprompt-lepton background are also taken into account. The nonprompt background is affected by the shape uncertainties arising from the dependence on the flavor composition of the jets misidentified as leptons. These shape uncertainties amount to $\approx$ 5–10% [72]. Statistical fluctuations in the data sets from which the scale factors are determined can be sizable in the $\ell\nu$qq analysis, with a 2–40% variation for electrons and 4–25% for muons. For the $2\ell2\nu$ channel, the trigger conditions are less tight, resulting in larger data sets for estimating efficiencies with negligible statistical uncertainties. In addition, a 30% normalization uncertainty is determined from a closure test performed with simulated samples.

The modeling of pileup depends on the total inelastic pp cross section [73]. The pileup uncertainty is evaluated by varying this cross section up and down by 5%. The uncertainty in the integrated luminosity measurement is 1.2, 2.3, and 2.5% for the 2016, 2017, and 2018 data sets, respectively [28–30], combining to an overall 1.6% uncertainty across the three years; it contributes directly to the normalization of the MC samples. Luminosity uncertainties are not considered for the top quark, W+jets, W^+W^-, and the DY background processes as their normalizations are determined by the fit to the data.

Several theoretical uncertainties are pertinent for all simulated event samples. Uncertainties in this category arise from the choice of PDFs and missing higher-order corrections in the perturbative expansion of the simulated cross sections. The PDF uncertainties are estimated, following the PDF4LHC recommendations [74], comparing the value obtained using the set of MC replicas provided by the NNPDF collaboration and PDFs with varied α_S values. The estimated uncertainties from missing higher-order corrections in the perturbative QCD expansion are given by the bin-by-bin difference between the nominal and alternative templates, which are constructed from simulated events, where renormalization and factorization scales are shifted up and down by a factor of two. The parton showering scale uncertainties are estimated by varying the initial-state and final-state radiation scales separately by a factor two. An overall 1.5% UE uncertainty is applied to all the simulated samples in order to account for fluctuations obtained from alternative MC simulations with UE tune variations [75].

Theoretical systematic uncertainties specific to individual background processes are also considered. A 15% uncertainty is applied to the relative fraction of the gluon-induced component of the W^+W^- background [76], while for the $q\bar{q} \to WW$ component, the applied p_T^{WW} corrections are varied by changing the renormalization and factorization scales. For the $t\bar{t}$ component in the t production background samples, the entire p_T correction weight (as mentioned in section 3) is treated as the uncertainty. Furthermore, the entire EW NLO correction to the W+jets samples is considered as an uncertainty, while variations in the QCD NLO corrections are estimated from statistical fluctuations in the sample sizes, and by varying the jet $|\eta|$ selections in the K factor estimations, resulting in 1 and 2% uncertainties, respectively. Differences in year-by-year setup for the W+jets simulation are addressed with an additional simulation-based nuisance parameter and amount to a ≈12% variation.

Finally, uncertainties arising from the limited statistical precision of the simulation are included for each bin of the discriminant distributions in each independent category [77]. In the $\ell\nu qq$ channel, these typically add an uncertainty of ≈ 20% in the highest BDT bins. For the $2\ell2\nu$ channel, the values vary greatly among the different analysis regions, typical values are ≈ 1–40% in SR1, ≈ 1–20% in SR2 and ≈ 1–10% in SR3.

9 Results

Distributions from the $2\ell2\nu$ and $\ell\nu qq$ channels are fitted jointly, and the signal is obtained from the results of the fit. These distributions correspond to both SRs and CRs.

For the $2\ell2\nu$ channel, the event yields in the CRs are recorded in single-bin histograms. Kinematic information from the SR is contained in two-dimensional distributions of $m_{\ell\ell}$ and $m_T^{\ell_{\min},p_T^{\text{miss}}}$. The $m_{\ell\ell}$ binning is [12, 60, 90, 120, ∞) GeV is chosen by taking into account the significance as a function of $m_{\ell\ell}$ for each dark Higgs boson mass. The $m_T^{\ell_{\min},p_T^{\text{miss}}}$ binning is chosen by optimizing the sensitivity to the different signal mass point distributions, subject to the requirements that bins that are more sensitive contain at least 10 events, and bins that are less sensitive contain at least 1 event in each data period: [0, 50, 90, 130, 160, ∞), [0, 50, 90,

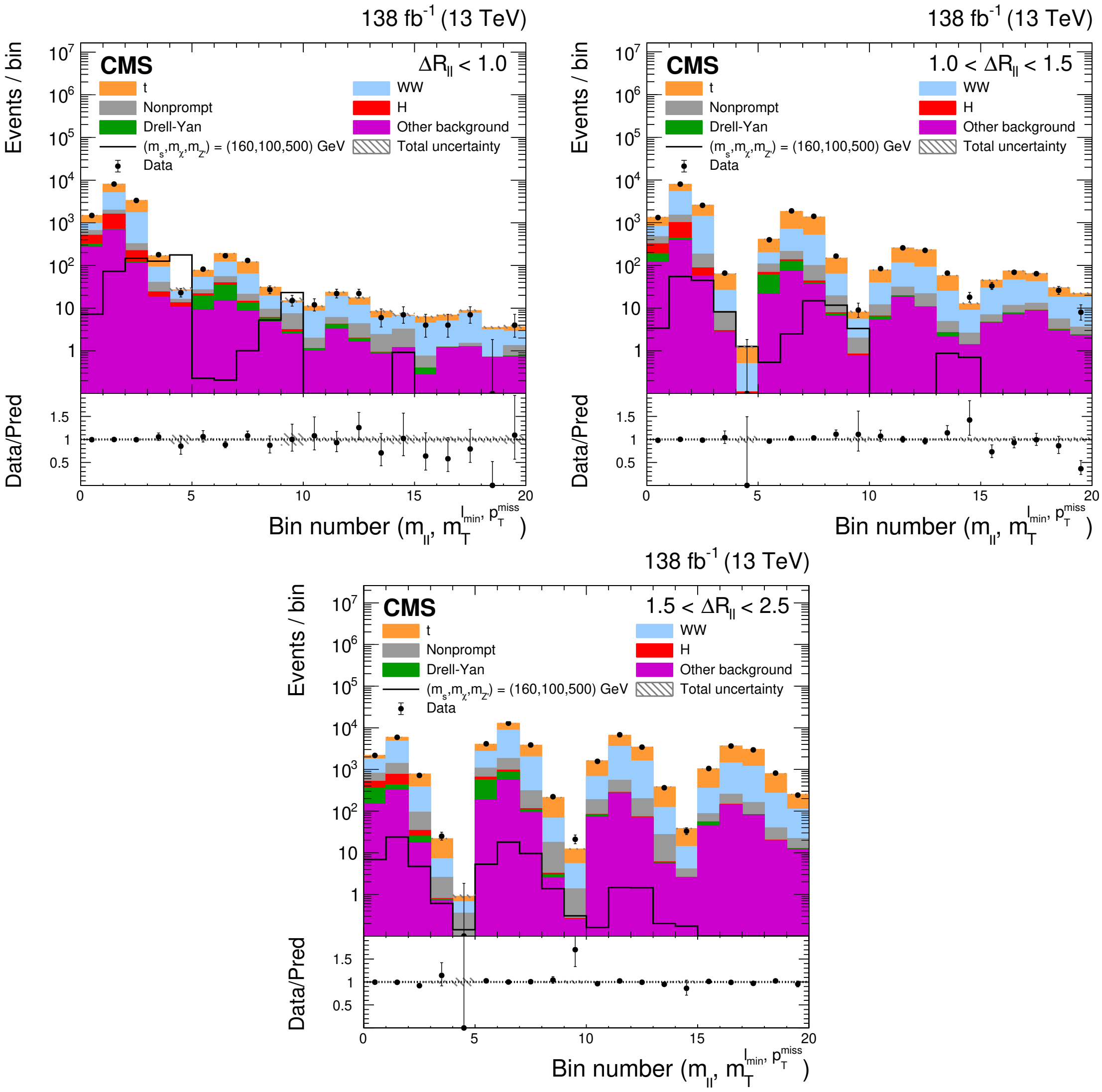

Figure 3. Unrolled ($m_{\ell\ell}$,$m_{\mathrm{T}}^{\ell_{\min},p_{\mathrm{T}}^{\mathrm{miss}}}$) post-fit distributions in the $2\ell 2\nu$ channel in a given $\Delta R_{\ell\ell}$ region SR1 (upper left), SR2 (upper right), and SR3 (lower), for the full data set. The histogram bins are spaced uniformly. Each group of five bins (from left to right) corresponds to the $m_{\mathrm{T}}^{\ell_{\min},p_{\mathrm{T}}^{\mathrm{miss}}}$ distribution in a $m_{\ell\ell}$ region, placed in ascending order. The black line indicates the signal prediction for $m_{\mathrm{s}} = 160\,\mathrm{GeV}$, $m_\chi = 100\,\mathrm{GeV}$, $m_{\mathrm{Z}'} = 500\,\mathrm{GeV}$. In the lower panel of each plot, the ratio between the data and the background prediction is shown.

130, 170, ∞), and [0, 50, 90, 130, 180, ∞) GeV for 2016, 2017, and 2018 data sets respectively. This strategy provides flexibility to the analysis, and allows the hypothetical signals to freely populate the ($\Delta R_{\ell\ell}$,$m_{\ell\ell}$,$m_{\mathrm{T}}^{\ell_{\min},p_{\mathrm{T}}^{\mathrm{miss}}}$) phase space according to the kinematic properties of the different dark Higgs boson mass points while establishing a uniform procedure for modeling background. In figure 3, the ($m_{\ell\ell}$,$m_{\mathrm{T}}^{\ell_{\min},p_{\mathrm{T}}^{\mathrm{miss}}}$) post-fit distributions for the full integrated luminosity of $138\,\mathrm{fb}^{-1}$ are unrolled into contiguous 1-dimensional slices showing the $m_{\mathrm{T}}^{\ell_{\min},p_{\mathrm{T}}^{\mathrm{miss}}}$ distributions for separate regions of $m_{\ell\ell}$. Post-fit expected background and data yields for the three SRs are listed in table 5.

Process	WW CR	DY CR	t quark CR	SR1	SR2	SR3
t quark	18000±510	953±38	347800±1300	5480±170	7090±210	21250±600
Nonprompt	3160±370	247±30	9600±1200	738±92	1050±120	3500±410
DY	240±11	2171±74	517±35	112.6±7.0	211±11	1042±48
WW	19250±660	517±36	3330±230	4980±200	6760±240	22480±710
VZ	28.3±1.0	27.0±1.4	29.4±1.8	24.29±0.97	28.8±1.0	63.8±2.4
$V\gamma + V\gamma^*$	1580±170	152±13	644±82	1088±96	703±74	1870±200
VVV	74.3±2.8	8.67±0.38	63.2±3.8	25.73±1.00	28.9±1.1	77.5±2.9
H	56.4±1.5	109.1±3.9	516±25	1202±29	759±19	712±18
Signal	3.409±0.097	3.119±0.081	70.0±2.4	561.8±6.5	147.1±1.7	74.30±0.76
Total bgnd	42390±190	4184±64	362520±600	13649±87	16634±84	50990±180
Data	42397	4183	362508	13627	16681	50918

Table 5. Data and background yields for each analysis region in the $2\ell 2\nu$ channel. Central values and uncertainties for the background contributions are the post-fit values. For the signal prediction from simulation, with the associated uncertainties, values are given for a sample with $m_s = 160\,\text{GeV}$, $m_\chi = 100\,\text{GeV}$, $m_{Z'} = 500\,\text{GeV}$.

In the $\ell\nu$qq channel, the signal and background information is contained in BDT distributions for the SRs and CRs. The binning is set by considering the bin-to-bin significance of dark Higgs boson mass points and by requiring the expected yield to be greater than 10 events in every bin. A coarser binning is obtained for the CRs and also for the 2016 SR ([−1, 0, 0.4, 0.6, 0.8, 1]) while a finer binning is obtained for the 2017–2018 SRs ([−1, 0, 0.4, 0.6, 0.7, 0.8, 0.9, 1]). The post-fit distributions of the SRs and CRs are shown in figure 4 for the two CRs (upper two plots corresponding to $138\,\text{fb}^{-1}$), the 2016 SR (lower left plot, $36.3\,\text{fb}^{-1}$) and the combined 2017–2018 SRs (lower right plot, $101\,\text{fb}^{-1}$). In the t quark CR and the 2017–2018 SR distributions shown in figure 4, a downward slope is visible in the last two bins of the distribution of the ratio of the observed to predicted events. This apparent trend is found to be an artifact of the chosen binning. Table 6 shows the post-fit expected yields of the background processes and the pre-fit signal for the sample with $m_s = 160\,\text{GeV}$, $m_\chi = 100\,\text{GeV}$, $m_{Z'} = 500\,\text{GeV}$, when the BDT discriminator values are above 0.6.

Neither the $2\ell 2\nu$ nor the $\ell\nu$qq channel show a significant deviation from the SM predictions. To extract upper limits, a modified frequentist approach was pursued using the CL_s criterion [78, 79]. Upper limits at 95% confidence level (CL) on the model production cross section are obtained from the combination of both final-states; these upper limits are displayed in the (m_s, $m_{Z'}$) mass plane in figure 5. An interpolation between the signal samples is carried out by reweighting the events using the ratio of dark Higgs boson p_T; the reweighted samples are rescaled according to the respective theoretical cross sections to obtain the correct kinematic distributions. A deficit of data events in the most sensitive bins, namely, the high-$m_T^{\ell_{\min}, p_T^{\text{miss}}}$ bins in the $2\ell 2\nu$ channel (with a local significance of 1.8 and 2.3 sigma in the highest $m_{\ell\ell}$ bin of SR1 and SR2) and the high-BDT bins in the $\ell\nu$qq channel (with a local significance of 1.8 sigma in the last SR bin of 2017–2018), leads to an observed limit that is more stringent than the expected one. The differences are not statistically significant, however, and the observed limit falls within two standard deviations of the expected one for most of

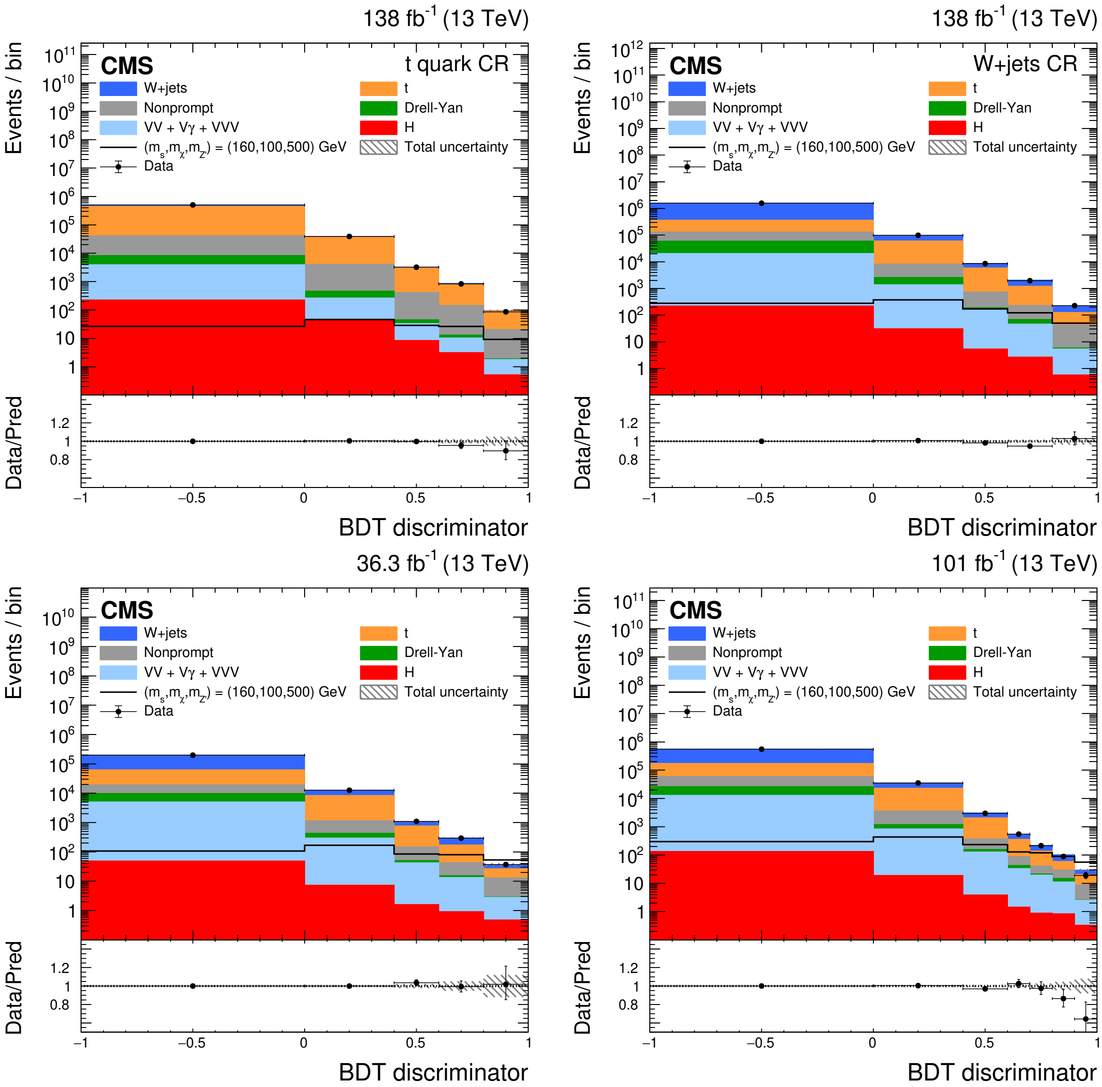

Figure 4. Post-fit BDT distributions in the $\ell\nu$qq channel for the full data set in the t quark CR (upper left) and W+jets CR (upper right). The SR of the 2016 data set (lower left) and the 2017–2018 data set (lower right). The black line indicates the signal prediction with $m_{\mathrm{s}} = 160\,\mathrm{GeV}$, $m_\chi = 100\,\mathrm{GeV}$, $m_{Z'} = 500\,\mathrm{GeV}$. In the lower panel of each plot, the ratio between the data and the background prediction is shown.

the scanned parameter space. For $m_\chi = 200\,\mathrm{GeV}$, near $m_{\mathrm{s}} = 350\,\mathrm{GeV}$ and $m_{Z'} = 700\,\mathrm{GeV}$, the observed exclusion limit is just over two standard deviations above the expected one.

Comparison with the observed DM relic density can indicate the preferred model parameters. Therefore, relic density calculations are performed with the current dark Higgs model assumptions using MadDM [80]. When the dark Higgs boson mass is lower than the DM mass, DM annihilation to two s bosons is on-shell, thereby reducing the relic density compared to models with only the Z′ boson as the mediator. In the case where $m_{\mathrm{s}} \approx 2m_\chi$, the WIMPs can be converted to SM particles through an on-shell dark Higgs resonance, strongly reducing the relic density. Gray lines in figure 5 indicate where the model parameters produce exactly the current measurement of the observed relic density [7].

Process	W+jets CR	t quark CR	SR
W+jets	916±42	52.0±5.0	461±27
t quark	1035±28	742±24	531±15
Nonprompt	201±27	142±23	124±18
DY	19.9±4.9	2.89±0.51	17.2±4.0
WW	23.3±2.7	4.70±0.51	44.6±3.4
VZ	0.190±0.015	0.682±0.055	0.371±0.024
$V\gamma + V\gamma^*$	22±12	0.78±0.13	13.4±4.4
VVV	3.81±0.16	1.62±0.13	8.91±0.60
H	3.09±0.15	3.61±0.18	4.71±0.21
Signal	172.2±3.3	35.5±2.1	528.1±9.3
Total background	2225±39	950±22	1205±29
Data	2179	917	1202

Table 6. Data and background yields for the $\ell\nu$qq channel with a BDT discriminator score above 0.6. Central values and uncertainties for the background contributions are the post-fit values. For the signal prediction from simulation, with the associated uncertainties, values are given for a sample with $m_\mathrm{s} = 160\,\mathrm{GeV}$, $m_\chi = 100\,\mathrm{GeV}$, $m_{Z'} = 500\,\mathrm{GeV}$.

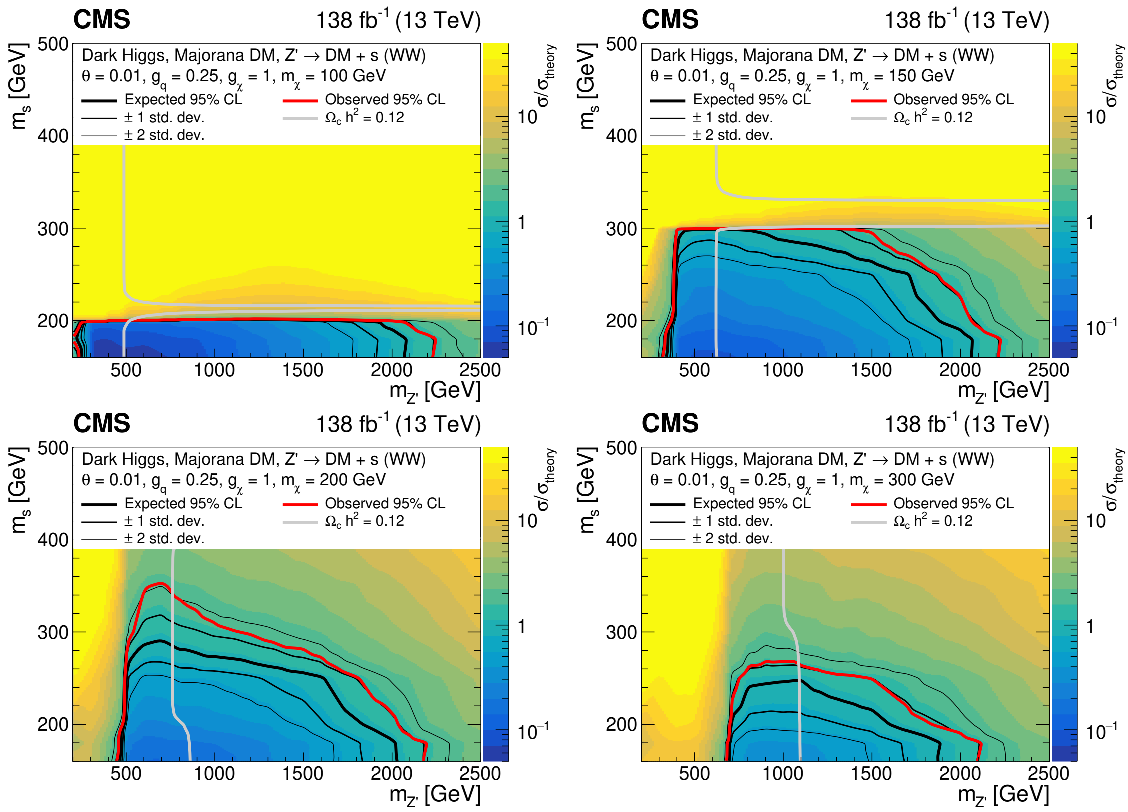

Figure 5. Observed (expected) exclusion regions at 95% CL for the dark Higgs model in the (m_s, $m_{Z'}$) plane, marked by the solid red (black) line. The expected $\pm1\sigma$ (68% CL) and $\pm2\sigma$ (95% CL) bands are shown as the thinner black lines. The bar on the righthand side of each figure maps the displayed colors to the corresponding limit values. Upper left: $m_\chi = 100\,\mathrm{GeV}$, upper right: $m_\chi = 150\,\mathrm{GeV}$, lower left: $m_\chi = 200\,\mathrm{GeV}$, lower right: $m_\chi = 300\,\mathrm{GeV}$. The gray line indicates were the model parameters produce exactly the observed relic density $\Omega_\mathrm{c}h^2 = 0.12$ [7].

JHEP03(2024)134

In this analysis, only the decay of the dark Higgs boson to a pair of visible W bosons is considered; this decay mode is dominant in the phase space analyzed. In the case where $m_\mathrm{s} > 2m_\chi$, however, the dark Higgs boson decays predominantly to a pair of DM particles. The consequence of this change of decay mode can be seen in figure 5: there is a boundary reflecting a sharp drop of sensitivity in the upper left (upper right) plot corresponding to m_s equal to twice the DM particle mass of 100 (150) GeV.

This search covers a wider range of DM mass (100–300 GeV) compared to previous analyses [23, 24]. In the (m_s, $m_{\mathrm{Z}'}$) plane with $m_\chi = 200$ GeV, $m_{\mathrm{Z}'}$ values up to ≈ 2200 GeV are excluded for m_s close to 160 GeV, extending the lower limit on $m_{\mathrm{Z}'}$ presented in ref. [24]. In the same plane, the lower limit on m_s is ≈ 350 GeV for $m_{\mathrm{Z}'}$ around 700 GeV, which is slightly weaker than that of ref. [24].

10 Summary

A search for dark matter particles χ produced in association with a dark Higgs boson (s) has been presented. Proton-proton collision data at a center-of-mass energy of 13 TeV are used, corresponding to an integrated luminosity of 138 fb^{-1}. The decay mode of the dark Higgs boson to a $\mathrm{W}^+\mathrm{W}^-$ pair is explored. Results are presented from a combination of the $2\ell 2\nu$ and $\ell\nu$qq decay channels of the $\mathrm{W}^+\mathrm{W}^-$ pair (where ℓ = electrons or muons). No significant deviation from the standard model prediction is observed. Upper limits at 95% confidence level on the production cross section for dark matter particles are set and translated into bounds on dark Higgs model parameters. This analysis investigates a dark matter mass range 100–300 GeV, which is wider than in previous searches and extends the limit on the Z′ boson mass $m_{\mathrm{Z}'}$ in the region of the s mass $160 < m_\mathrm{s} \lesssim 250$ GeV for $m_\chi = 200$ GeV. The most stringent limit is set for $m_\chi = 200$ GeV, excluding m_s masses up to ≈ 350 GeV at $m_{\mathrm{Z}'} = 700$ GeV, and up to $m_{\mathrm{Z}'} \approx 2200$ GeV for $m_\mathrm{s} = 160$ GeV.

Acknowledgments

We congratulate our colleagues in the CERN accelerator departments for the excellent performance of the LHC and thank the technical and administrative staffs at CERN and at other CMS institutes for their contributions to the success of the CMS effort. In addition, we gratefully acknowledge the computing centers and personnel of the Worldwide LHC Computing Grid and other centers for delivering so effectively the computing infrastructure essential to our analyses. Finally, we acknowledge the enduring support for the construction and operation of the LHC, the CMS detector, and the supporting computing infrastructure provided by the following funding agencies: SC (Armenia), BMBWF and FWF (Austria); FNRS and FWO (Belgium); CNPq, CAPES, FAPERJ, FAPERGS, and FAPESP (Brazil); MES and BNSF (Bulgaria); CERN; CAS, MoST, and NSFC (China); MINCIENCIAS (Colombia); MSES and CSF (Croatia); RIF (Cyprus); SENESCYT (Ecuador); MoER, ERC PUT and ERDF (Estonia); Academy of Finland, MEC, and HIP (Finland); CEA and CNRS/IN2P3 (France); SRNSF (Georgia); BMBF, DFG, and HGF (Germany); GSRI (Greece); NKFIH (Hungary); DAE and DST (India); IPM (Iran); SFI (Ireland); INFN (Italy); MSIP and NRF (Republic of Korea); MES (Latvia); LAS (Lithuania); MOE and UM (Malaysia); BUAP,

JHEP03(2024)134

CINVESTAV, CONACYT, LNS, SEP, and UASLP-FAI (Mexico); MOS (Montenegro); MBIE (New Zealand); PAEC (Pakistan); MES and NSC (Poland); FCT (Portugal); MESTD (Serbia); MCIN/AEI and PCTI (Spain); MOSTR (Sri Lanka); Swiss Funding Agencies (Switzerland); MST (Taipei); MHESI and NSTDA (Thailand); TUBITAK and TENMAK (Turkey); NASU (Ukraine); STFC (United Kingdom); DOE and NSF (USA).

Individuals have received support from the Marie-Curie program and the European Research Council and Horizon 2020 Grant, contract Nos. 675440, 724704, 752730, 758316, 765710, 824093, and COST Action CA16108 (European Union); the Leventis Foundation; the Alfred P. Sloan Foundation; the Alexander von Humboldt Foundation; the Science Committee, project no. 22rl-037 (Armenia); the Belgian Federal Science Policy Office; the Fonds pour la Formation à la Recherche dans l'Industrie et dans l'Agriculture (FRIA-Belgium); the Agentschap voor Innovatie door Wetenschap en Technologie (IWT-Belgium); the F.R.S.-FNRS and FWO (Belgium) under the "Excellence of Science — EOS" — be.h project n. 30820817; the Beijing Municipal Science & Technology Commission, No. Z191100007219010 and Fundamental Research Funds for the Central Universities (China); the Ministry of Education, Youth and Sports (MEYS) of the Czech Republic; the Shota Rustaveli National Science Foundation, grant FR-22-985 (Georgia); the Deutsche Forschungsgemeinschaft (DFG), under Germany's Excellence Strategy — EXC 2121 "Quantum Universe" — 390833306, and under project number 400140256 - GRK2497; the Hellenic Foundation for Research and Innovation (HFRI), Project Number 2288 (Greece); the Hungarian Academy of Sciences, the New National Excellence Program - ÚNKP, the NKFIH research grants K 124845, K 124850, K 128713, K 128786, K 129058, K 131991, K 133046, K 138136, K 143460, K 143477, 2020-2.2.1-ED-2021-00181, and TKP2021-NKTA-64 (Hungary); the Council of Science and Industrial Research, India; ICSC — National Research Center for High Performance Computing, Big Data and Quantum Computing, funded by the EU NexGeneration program (Italy); the Latvian Council of Science; the Ministry of Education and Science, project no. 2022/WK/14, and the National Science Center, contracts Opus 2021/41/B/ST2/01369 and 2021/43/B/ST2/01552 (Poland); the Fundação para a Ciência e a Tecnologia, grant CEECIND/01334/2018 (Portugal); the National Priorities Research Program by Qatar National Research Fund; MCIN/AEI/10.13039/501100011033, ERDF "a way of making Europe", and the Programa Estatal de Fomento de la Investigación Científica y Técnica de Excelencia María de Maeztu, grant MDM-2017-0765 and Programa Severo Ochoa del Principado de Asturias (Spain); the Chulalongkorn Academic into Its 2nd Century Project Advancement Project, and the National Science, Research and Innovation Fund via the Program Management Unit for Human Resources & Institutional Development, Research and Innovation, grant B05F650021 (Thailand); the Kavli Foundation; the Nvidia Corporation; the SuperMicro Corporation; the Welch Foundation, contract C-1845; and the Weston Havens Foundation (USA).

References

[1] R.J. Gaitskell, *Direct detection of dark matter*, *Ann. Rev. Nucl. Part. Sci.* **54** (2004) 315 [INSPIRE].

[2] V. Trimble, *Existence and Nature of Dark Matter in the Universe*, *Ann. Rev. Astron. Astrophys.* **25** (1987) 425 [INSPIRE].

[3] T.A. Porter, R.P. Johnson and P.W. Graham, *Dark Matter Searches with Astroparticle Data*, *Ann. Rev. Astron. Astrophys.* **49** (2011) 155 [arXiv:1104.2836] [INSPIRE].

[4] G. Bertone, D. Hooper and J. Silk, *Particle dark matter: evidence, candidates and constraints*, *Phys. Rept.* **405** (2005) 279 [hep-ph/0404175] [INSPIRE].

[5] J.L. Feng, *Dark Matter Candidates from Particle Physics and Methods of Detection*, *Ann. Rev. Astron. Astrophys.* **48** (2010) 495 [arXiv:1003.0904] [INSPIRE].

[6] R.J. Scherrer and M.S. Turner, *On the Relic, Cosmic Abundance of Stable Weakly Interacting Massive Particles*, *Phys. Rev. D* **33** (1986) 1585 [*Erratum ibid.* **34** (1986) 3263] [INSPIRE].

[7] PLANCK collaboration, *Planck 2018 results. VI. Cosmological parameters*, *Astron. Astrophys.* **641** (2020) A6 [*Erratum ibid.* **652** (2021) C4] [arXiv:1807.06209] [INSPIRE].

[8] G. Steigman and M.S. Turner, *Cosmological Constraints on the Properties of Weakly Interacting Massive Particles*, *Nucl. Phys. B* **253** (1985) 375 [INSPIRE].

[9] ATLAS collaboration, *Search for dark matter and other new phenomena in events with an energetic jet and large missing transverse momentum using the ATLAS detector*, *JHEP* **01** (2018) 126 [arXiv:1711.03301] [INSPIRE].

[10] CMS collaboration, *Search for new physics in final states with an energetic jet or a hadronically decaying W or Z boson and transverse momentum imbalance at $\sqrt{s} = 13\,\text{TeV}$*, *Phys. Rev. D* **97** (2018) 092005 [arXiv:1712.02345] [INSPIRE].

[11] ATLAS collaboration, *Search for dark matter produced in association with bottom or top quarks in $\sqrt{s} = 13$ TeV pp collisions with the ATLAS detector*, *Eur. Phys. J. C* **78** (2018) 18 [arXiv:1710.11412] [INSPIRE].

[12] CMS collaboration, *Search for dark matter in events with energetic, hadronically decaying top quarks and missing transverse momentum at $\sqrt{s} = 13$ TeV*, *JHEP* **06** (2018) 027 [arXiv:1801.08427] [INSPIRE].

[13] ATLAS collaboration, *Search for dark matter at $\sqrt{s} = 13$ TeV in final states containing an energetic photon and large missing transverse momentum with the ATLAS detector*, *Eur. Phys. J. C* **77** (2017) 393 [arXiv:1704.03848] [INSPIRE].

[14] CMS collaboration, *Search for new physics in the monophoton final state in proton-proton collisions at $\sqrt{s} = 13$ TeV*, *JHEP* **10** (2017) 073 [arXiv:1706.03794] [INSPIRE].

[15] ATLAS collaboration, *Search for an invisibly decaying Higgs boson or dark matter candidates produced in association with a Z boson in pp collisions at $\sqrt{s} = 13$ TeV with the ATLAS detector*, *Phys. Lett. B* **776** (2018) 318 [arXiv:1708.09624] [INSPIRE].

[16] CMS collaboration, *Search for new physics in events with a leptonically decaying Z boson and a large transverse momentum imbalance in proton–proton collisions at $\sqrt{s} = 13$ TeV*, *Eur. Phys. J. C* **78** (2018) 291 [arXiv:1711.00431] [INSPIRE].

[17] ATLAS collaboration, *Search for dark matter in events with a hadronically decaying vector boson and missing transverse momentum in pp collisions at $\sqrt{s} = 13$ TeV with the ATLAS detector*, *JHEP* **10** (2018) 180 [arXiv:1807.11471] [INSPIRE].

[18] CMS collaboration, *Search for dark matter particles produced in association with a Higgs boson in proton-proton collisions at* $\sqrt{s} = 13$ *TeV*, *JHEP* **03** (2020) 025 [arXiv:1908.01713] [INSPIRE].

[19] M. Duerr et al., *Hunting the dark Higgs*, *JHEP* **04** (2017) 143 [arXiv:1701.08780] [INSPIRE].

[20] M. Duerr et al., *How to save the WIMP: global analysis of a dark matter model with two s-channel mediators*, *JHEP* **09** (2016) 042 [arXiv:1606.07609] [INSPIRE].

[21] N.F. Bell, Y. Cai and R.K. Leane, *Dark Forces in the Sky: Signals from* Z' *and the Dark Higgs*, *JCAP* **08** (2016) 001 [arXiv:1605.09382] [INSPIRE].

[22] ATLAS collaboration, *RECAST framework reinterpretation of an ATLAS Dark Matter Search constraining a model of a dark Higgs boson decaying to two b-quarks*, ATL-PHYS-PUB-2019-032, CERN, Geneva (2019).

[23] ATLAS collaboration, *Search for Dark Matter Produced in Association with a Dark Higgs Boson Decaying into* $W^{\pm}W^{\mp}$ *or* ZZ *in Fully Hadronic Final States from* $\sqrt{s} = 13$ *TeV pp Collisions Recorded with the ATLAS Detector*, *Phys. Rev. Lett.* **126** (2021) 121802 [arXiv:2010.06548] [INSPIRE].

[24] ATLAS collaboration, *Search for dark matter produced in association with a dark Higgs boson decaying into* W^+W^- *in the one-lepton final state at* $\sqrt{s} = 13$ *TeV using* $139\,fb^{-1}$ *of pp collisions recorded with the ATLAS detector*, *JHEP* **07** (2023) 116 [arXiv:2211.07175] [INSPIRE].

[25] HEPData record for this analysis, http://dx.doi.org/10.17182/hepdata.139719 (2023).

[26] CMS collaboration, *The CMS trigger system*, 2017 *JINST* **12** P01020 [arXiv:1609.02366] [INSPIRE].

[27] CMS collaboration, *The CMS Experiment at the CERN LHC*, 2008 *JINST* **3** S08004 [INSPIRE].

[28] CMS collaboration, *Precision luminosity measurement in proton-proton collisions at* $\sqrt{s} = 13$ *TeV in 2015 and 2016 at CMS*, *Eur. Phys. J. C* **81** (2021) 800 [arXiv:2104.01927] [INSPIRE].

[29] CMS collaboration, *CMS luminosity measurement for the 2017 data-taking period at* $\sqrt{s} = 13$ TeV, CMS-PAS-LUM-17-004, CERN, Geneva (2018).

[30] CMS collaboration, *CMS luminosity measurement for the 2018 data-taking period at* $\sqrt{s} = 13$ TeV, CMS-PAS-LUM-18-002, CERN, Geneva (2019).

[31] T. Sjöstrand et al., *An introduction to PYTHIA 8.2*, *Comput. Phys. Commun.* **191** (2015) 159 [arXiv:1410.3012] [INSPIRE].

[32] CMS collaboration, *Event generator tunes obtained from underlying event and multiparton scattering measurements*, *Eur. Phys. J. C* **76** (2016) 155 [arXiv:1512.00815] [INSPIRE].

[33] CMS collaboration, *Extraction and validation of a new set of CMS PYTHIA8 tunes from underlying-event measurements*, *Eur. Phys. J. C* **80** (2020) 4 [arXiv:1903.12179] [INSPIRE].

[34] NNPDF collaboration, *Parton distributions with QED corrections*, *Nucl. Phys. B* **877** (2013) 290 [arXiv:1308.0598] [INSPIRE].

[35] NNPDF collaboration, *Unbiased global determination of parton distributions and their uncertainties at NNLO and at LO*, *Nucl. Phys. B* **855** (2012) 153 [arXiv:1107.2652] [INSPIRE].

[36] NNPDF collaboration, *Parton distributions from high-precision collider data*, *Eur. Phys. J. C* **77** (2017) 663 [arXiv:1706.00428] [INSPIRE].

[37] J. Alwall et al., *The automated computation of tree-level and next-to-leading order differential cross sections, and their matching to parton shower simulations*, *JHEP* **07** (2014) 079 [arXiv:1405.0301] [INSPIRE].

[38] D. Abercrombie et al., *Dark Matter benchmark models for early LHC Run-2 Searches: Report of the ATLAS/CMS Dark Matter Forum*, *Phys. Dark Univ.* **27** (2020) 100371 [arXiv:1507.00966] [INSPIRE].

[39] T. Melia, P. Nason, R. Rontsch and G. Zanderighi, *W^+W^-, WZ and ZZ production in the POWHEG BOX*, *JHEP* **11** (2011) 078 [arXiv:1107.5051] [INSPIRE].

[40] J.M. Campbell, R.K. Ellis and C. Williams, *Vector Boson Pair Production at the LHC*, *JHEP* **07** (2011) 018 [arXiv:1105.0020] [INSPIRE].

[41] J.M. Campbell, R.K. Ellis and W.T. Giele, *A Multi-Threaded Version of MCFM*, *Eur. Phys. J. C* **75** (2015) 246 [arXiv:1503.06182] [INSPIRE].

[42] P. Meade, H. Ramani and M. Zeng, *Transverse momentum resummation effects in W^+W^- measurements*, *Phys. Rev. D* **90** (2014) 114006 [arXiv:1407.4481] [INSPIRE].

[43] P. Jaiswal and T. Okui, *Explanation of the WW excess at the LHC by jet-veto resummation*, *Phys. Rev. D* **90** (2014) 073009 [arXiv:1407.4537] [INSPIRE].

[44] S. Gieseke, T. Kasprzik and J.H. Kühn, *Vector-boson pair production and electroweak corrections in HERWIG++*, *Eur. Phys. J. C* **74** (2014) 2988 [arXiv:1401.3964] [INSPIRE].

[45] F. Caola, K. Melnikov, R. Röntsch and L. Tancredi, *QCD corrections to W^+W^- production through gluon fusion*, *Phys. Lett. B* **754** (2016) 275 [arXiv:1511.08617] [INSPIRE].

[46] P. Nason, *A New method for combining NLO QCD with shower Monte Carlo algorithms*, *JHEP* **11** (2004) 040 [hep-ph/0409146] [INSPIRE].

[47] S. Frixione, P. Nason and C. Oleari, *Matching NLO QCD computations with Parton Shower simulations: the POWHEG method*, *JHEP* **11** (2007) 070 [arXiv:0709.2092] [INSPIRE].

[48] S. Alioli, P. Nason, C. Oleari and E. Re, *A general framework for implementing NLO calculations in shower Monte Carlo programs: the POWHEG BOX*, *JHEP* **06** (2010) 043 [arXiv:1002.2581] [INSPIRE].

[49] E. Bagnaschi, G. Degrassi, P. Slavich and A. Vicini, *Higgs production via gluon fusion in the POWHEG approach in the SM and in the MSSM*, *JHEP* **02** (2012) 088 [arXiv:1111.2854] [INSPIRE].

[50] P. Nason and C. Oleari, *NLO Higgs boson production via vector-boson fusion matched with shower in POWHEG*, *JHEP* **02** (2010) 037 [arXiv:0911.5299] [INSPIRE].

[51] G. Luisoni, P. Nason, C. Oleari and F. Tramontano, *$HW^\pm/HZ + 0$ and 1 jet at NLO with the POWHEG BOX interfaced to GoSam and their merging within MiNLO*, *JHEP* **10** (2013) 083 [arXiv:1306.2542] [INSPIRE].

[52] H.B. Hartanto, B. Jager, L. Reina and D. Wackeroth, *Higgs boson production in association with top quarks in the POWHEG BOX*, *Phys. Rev. D* **91** (2015) 094003 [arXiv:1501.04498] [INSPIRE].

[53] S. Bolognesi et al., *On the Spin and Parity of a Single-Produced Resonance at the LHC*, *Phys. Rev. D* **86** (2012) 095031 [arXiv:1208.4018] [INSPIRE].

[54] M. Czakon et al., *Top-pair production at the LHC through NNLO QCD and NLO EW*, *JHEP* **10** (2017) 186 [arXiv:1705.04105] [INSPIRE].

JHEP03(2024)134

[55] J.M. Lindert et al., *Precise predictions for V+ jets dark matter backgrounds*, *Eur. Phys. J. C* **77** (2017) 829 [arXiv:1705.04664] [INSPIRE].

[56] K. Melnikov and F. Petriello, *Electroweak gauge boson production at hadron colliders through $O(\alpha_s^2)$*, *Phys. Rev. D* **74** (2006) 114017 [hep-ph/0609070] [INSPIRE].

[57] GEANT4 collaboration, *GEANT4 — a simulation toolkit*, *Nucl. Instrum. Meth. A* **506** (2003) 250 [INSPIRE].

[58] D. Contardo et al., *Technical Proposal for the Phase-II Upgrade of the CMS Detector*, CERN-LHCC-2015-010 (2015) [DOI:10.17181/CERN.VU8I.D59J].

[59] CMS collaboration, *Particle-flow reconstruction and global event description with the CMS detector*, 2017 *JINST* **12** P10003 [arXiv:1706.04965] [INSPIRE].

[60] CMS collaboration, *Performance of Electron Reconstruction and Selection with the CMS Detector in Proton-Proton Collisions at $\sqrt{s} = 8$ TeV*, 2015 *JINST* **10** P06005 [arXiv:1502.02701] [INSPIRE].

[61] CMS collaboration, *Performance of the CMS muon detector and muon reconstruction with proton-proton collisions at $\sqrt{s} = 13$ TeV*, 2018 *JINST* **13** P06015 [arXiv:1804.04528] [INSPIRE].

[62] CMS collaboration, *Performance of the reconstruction and identification of high-momentum muons in proton-proton collisions at $\sqrt{s} = 13$ TeV*, 2020 *JINST* **15** P02027 [arXiv:1912.03516] [INSPIRE].

[63] M. Cacciari, G.P. Salam and G. Soyez, *The anti-k_t jet clustering algorithm*, *JHEP* **04** (2008) 063 [arXiv:0802.1189] [INSPIRE].

[64] M. Cacciari, G.P. Salam and G. Soyez, *FastJet User Manual*, *Eur. Phys. J. C* **72** (2012) 1896 [arXiv:1111.6097] [INSPIRE].

[65] CMS collaboration, *Jet algorithms performance in 13 TeV data*, CMS-PAS-JME-16-003, CERN, Geneva (2017).

[66] CMS collaboration, *Jet energy scale and resolution in the CMS experiment in pp collisions at 8 TeV*, 2017 *JINST* **12** P02014 [arXiv:1607.03663] [INSPIRE].

[67] CMS collaboration, *Identification of heavy-flavour jets with the CMS detector in pp collisions at 13 TeV*, 2018 *JINST* **13** P05011 [arXiv:1712.07158] [INSPIRE].

[68] CMS collaboration, *Performance of missing transverse momentum reconstruction in proton-proton collisions at $\sqrt{s} = 13$ TeV using the CMS detector*, 2019 *JINST* **14** P07004 [arXiv:1903.06078] [INSPIRE].

[69] D. Bertolini, P. Harris, M. Low and N. Tran, *Pileup Per Particle Identification*, *JHEP* **10** (2014) 059 [arXiv:1407.6013] [INSPIRE].

[70] L. Moneta et al., *The RooStats Project*, *PoS* **ACAT2010** (2010) 057 [arXiv:1009.1003] [INSPIRE].

[71] G. Cowan, K. Cranmer, E. Gross and O. Vitells, *Asymptotic formulae for likelihood-based tests of new physics*, *Eur. Phys. J. C* **71** (2011) 1554 [*Erratum ibid.* **73** (2013) 2501] [arXiv:1007.1727] [INSPIRE].

[72] CMS collaboration, *Measurements of properties of the Higgs boson decaying to a W boson pair in pp collisions at $\sqrt{s} = 13$ TeV*, *Phys. Lett. B* **791** (2019) 96 [arXiv:1806.05246] [INSPIRE].

[73] CMS collaboration, *Measurement of the inelastic proton-proton cross section at $\sqrt{s} = 13$ TeV*, *JHEP* **07** (2018) 161 [arXiv:1802.02613] [INSPIRE].

[74] J. Butterworth et al., *PDF4LHC recommendations for LHC Run II*, *J. Phys. G* **43** (2016) 023001 [arXiv:1510.03865] [INSPIRE].

[75] CMS collaboration, *Measurements of the Higgs boson production cross section and couplings in the W boson pair decay channel in proton-proton collisions at $\sqrt{s} = 13\,TeV$*, *Eur. Phys. J. C* **83** (2023) 667 [arXiv:2206.09466] [INSPIRE].

[76] F. Caola et al., *QCD corrections to vector boson pair production in gluon fusion including interference effects with off-shell Higgs at the LHC*, *JHEP* **07** (2016) 087 [arXiv:1605.04610] [INSPIRE].

[77] R.J. Barlow and C. Beeston, *Fitting using finite Monte Carlo samples*, *Comput. Phys. Commun.* **77** (1993) 219 [INSPIRE].

[78] T. Junk, *Confidence level computation for combining searches with small statistics*, *Nucl. Instrum. Meth. A* **434** (1999) 435 [hep-ex/9902006] [INSPIRE].

[79] A.L. Read, *Presentation of search results: The CL_s technique*, *J. Phys. G* **28** (2002) 2693 [INSPIRE].

[80] C. Arina et al., *Indirect dark-matter detection with MadDM v3.2 — Lines and Loops*, *Eur. Phys. J. C* **83** (2023) 241 [arXiv:2107.04598] [INSPIRE].

JHEP03(2024)134

The CMS collaboration

Yerevan Physics Institute, Yerevan, Armenia
A. Hayrapetyan, A. Tumasyan[1]

Institut für Hochenergiephysik, Vienna, Austria
W. Adam, J.W. Andrejkovic, T. Bergauer, S. Chatterjee, K. Damanakis, M. Dragicevic, A. Escalante Del Valle, P.S. Hussain, M. Jeitler[2], N. Krammer, D. Liko, I. Mikulec, J. Schieck[2], R. Schöfbeck, D. Schwarz, M. Sonawane, S. Templ, W. Waltenberger, C.-E. Wulz[2]

Universiteit Antwerpen, Antwerpen, Belgium
M.R. Darwish[3], T. Janssen, P. Van Mechelen

Vrije Universiteit Brussel, Brussel, Belgium
E.S. Bols, J. D'Hondt, S. Dansana, A. De Moor, M. Delcourt, H. El Faham, S. Lowette, I. Makarenko, D. Müller, A.R. Sahasransu, S. Tavernier, M. Tytgat[4], S. Van Putte, D. Vannerom

Université Libre de Bruxelles, Bruxelles, Belgium
B. Clerbaux, G. De Lentdecker, L. Favart, D. Hohov, J. Jaramillo, A. Khalilzadeh, K. Lee, M. Mahdavikhorrami, A. Malara, S. Paredes, L. Pétré, N. Postiau, L. Thomas, M. Vanden Bemden, C. Vander Velde, P. Vanlaer

Ghent University, Ghent, Belgium
M. De Coen, D. Dobur, Y. Hong, J. Knolle, L. Lambrecht, G. Mestdach, C. Rendón, A. Samalan, K. Skovpen, N. Van Den Bossche, L. Wezenbeek

Université Catholique de Louvain, Louvain-la-Neuve, Belgium
A. Benecke, G. Bruno, C. Caputo, C. Delaere, I.S. Donertas, A. Giammanco, K. Jaffel, Sa. Jain, V. Lemaitre, J. Lidrych, P. Mastrapasqua, K. Mondal, T.T. Tran, S. Wertz

Centro Brasileiro de Pesquisas Fisicas, Rio de Janeiro, Brazil
G.A. Alves, E. Coelho, C. Hensel, T. Menezes De Oliveira, A. Moraes, P. Rebello Teles, M. Soeiro

Universidade do Estado do Rio de Janeiro, Rio de Janeiro, Brazil
W.L. Aldá Júnior, M. Alves Gallo Pereira, M. Barroso Ferreira Filho, H. Brandao Malbouisson, W. Carvalho, J. Chinellato[5], E.M. Da Costa, G.G. Da Silveira[6], D. De Jesus Damiao, S. Fonseca De Souza, J. Martins[7], C. Mora Herrera, K. Mota Amarilo, L. Mundim, H. Nogima, A. Santoro, S.M. Silva Do Amaral, A. Sznajder, M. Thiel, A. Vilela Pereira

Universidade Estadual Paulista, Universidade Federal do ABC, São Paulo, Brazil
C.A. Bernardes[6], L. Calligaris, T.R. Fernandez Perez Tomei, E.M. Gregores, P.G. Mercadante, S.F. Novaes, B. Orzari, Sandra S. Padula

JHEP03(2024)134

Institute for Nuclear Research and Nuclear Energy, Bulgarian Academy of Sciences, Sofia, Bulgaria
A. Aleksandrov, G. Antchev, R. Hadjiiska, P. Iaydjiev, M. Misheva, M. Shopova, G. Sultanov

University of Sofia, Sofia, Bulgaria
A. Dimitrov, T. Ivanov, L. Litov, B. Pavlov, P. Petkov, A. Petrov, E. Shumka

Instituto De Alta Investigación, Universidad de Tarapacá, Casilla 7 D, Arica, Chile
S. Keshri, S. Thakur

Beihang University, Beijing, China
T. Cheng, Q. Guo, T. Javaid, M. Mittal, L. Yuan

Department of Physics, Tsinghua University, Beijing, China
G. Bauer[8], Z. Hu, K. Yi[8,9]

Institute of High Energy Physics, Beijing, China
G.M. Chen[10], H.S. Chen[10], M. Chen[10], F. Iemmi, C.H. Jiang, A. Kapoor, H. Liao, Z.-A. Liu[11], F. Monti, R. Sharma, J.N. Song[11], J. Tao, C. Wang[10], J. Wang, Z. Wang, H. Zhang

State Key Laboratory of Nuclear Physics and Technology, Peking University, Beijing, China
A. Agapitos, Y. Ban, A. Levin, C. Li, Q. Li, X. Lyu, Y. Mao, S.J. Qian, X. Sun, D. Wang, H. Yang, C. Zhou

Sun Yat-Sen University, Guangzhou, China
Z. You

University of Science and Technology of China, Hefei, China
N. Lu

Institute of Modern Physics and Key Laboratory of Nuclear Physics and Ion-beam Application (MOE) - Fudan University, Shanghai, China
D. Leggat, H. Okawa, Y. Zhang

Zhejiang University, Hangzhou, Zhejiang, China
Z. Lin, C. Lu, M. Xiao

Universidad de Los Andes, Bogota, Colombia
C. Avila, D.A. Barbosa Trujillo, A. Cabrera, C. Florez, J. Fraga, J.A. Reyes Vega

Universidad de Antioquia, Medellin, Colombia
J. Mejia Guisao, F. Ramirez, M. Rodriguez, J.D. Ruiz Alvarez

University of Split, Faculty of Electrical Engineering, Mechanical Engineering and Naval Architecture, Split, Croatia
D. Giljanovic, N. Godinovic, D. Lelas, A. Sculac

University of Split, Faculty of Science, Split, Croatia
M. Kovac, T. Sculac

Institute Rudjer Boskovic, Zagreb, Croatia
P. Bargassa, V. Brigljevic, B.K. Chitroda, D. Ferencek, S. Mishra, A. Starodumov[12], T. Susa

University of Cyprus, Nicosia, Cyprus
A. Attikis, K. Christoforou, S. Konstantinou, J. Mousa, C. Nicolaou, F. Ptochos, P.A. Razis, H. Rykaczewski, H. Saka, A. Stepennov

Charles University, Prague, Czech Republic
M. Finger, M. Finger Jr., A. Kveton

Escuela Politecnica Nacional, Quito, Ecuador
E. Ayala

Universidad San Francisco de Quito, Quito, Ecuador
E. Carrera Jarrin

Academy of Scientific Research and Technology of the Arab Republic of Egypt, Egyptian Network of High Energy Physics, Cairo, Egypt
S. Elgammal[13], A. Ellithi Kamel[14]

Center for High Energy Physics (CHEP-FU), Fayoum University, El-Fayoum, Egypt
A. Lotfy, M.A. Mahmoud

National Institute of Chemical Physics and Biophysics, Tallinn, Estonia
R.K. Dewanjee[15], K. Ehataht, M. Kadastik, T. Lange, S. Nandan, C. Nielsen, J. Pata, M. Raidal, L. Tani, C. Veelken

Department of Physics, University of Helsinki, Helsinki, Finland
H. Kirschenmann, K. Osterberg, M. Voutilainen

Helsinki Institute of Physics, Helsinki, Finland
S. Bharthuar, E. Brücken, F. Garcia, J. Havukainen, K.T.S. Kallonen, M.S. Kim, R. Kinnunen, T. Lampén, K. Lassila-Perini, S. Lehti, T. Lindén, M. Lotti, L. Martikainen, M. Myllymäki, M.m. Rantanen, H. Siikonen, E. Tuominen, J. Tuominiemi

Lappeenranta-Lahti University of Technology, Lappeenranta, Finland
P. Luukka, H. Petrow, T. Tuuva[†]

JHEP03(2024)134

IRFU, CEA, Université Paris-Saclay, Gif-sur-Yvette, France
M. Besancon, F. Couderc, M. Dejardin, D. Denegri, J.L. Faure, F. Ferri, S. Ganjour, P. Gras, G. Hamel de Monchenault, V. Lohezic, J. Malcles, J. Rander, A. Rosowsky, M.Ö. Sahin, A. Savoy-Navarro[16], P. Simkina, M. Titov

Laboratoire Leprince-Ringuet, CNRS/IN2P3, Ecole Polytechnique, Institut Polytechnique de Paris, Palaiseau, France
C. Baldenegro Barrera, F. Beaudette, A. Buchot Perraguin, P. Busson, A. Cappati, C. Charlot, F. Damas, O. Davignon, A. De Wit, G. Falmagne, B.A. Fontana Santos Alves, S. Ghosh, A. Gilbert, R. Granier de Cassagnac, A. Hakimi, B. Harikrishnan, L. Kalipoliti, G. Liu, J. Motta, M. Nguyen, C. Ochando, L. Portales, R. Salerno, U. Sarkar, J.B. Sauvan, Y. Sirois, A. Tarabini, E. Vernazza, A. Zabi, A. Zghiche

Université de Strasbourg, CNRS, IPHC UMR 7178, Strasbourg, France
J.-L. Agram[17], J. Andrea, D. Apparu, D. Bloch, J.-M. Brom, E.C. Chabert, C. Collard, S. Falke, U. Goerlach, C. Grimault, R. Haeberle, A.-C. Le Bihan, M.A. Sessini, P. Van Hove

Institut de Physique des 2 Infinis de Lyon (IP2I), Villeurbanne, France
S. Beauceron, B. Blancon, G. Boudoul, N. Chanon, J. Choi, D. Contardo, P. Depasse, C. Dozen[18], H. El Mamouni, J. Fay, S. Gascon, M. Gouzevitch, C. Greenberg, G. Grenier, B. Ille, I.B. Laktineh, M. Lethuillier, L. Mirabito, S. Perries, M. Vander Donckt, P. Verdier, J. Xiao

Georgian Technical University, Tbilisi, Georgia
G. Adamov, I. Lomidze, Z. Tsamalaidze[12]

RWTH Aachen University, I. Physikalisches Institut, Aachen, Germany
V. Botta, L. Feld, K. Klein, M. Lipinski, D. Meuser, A. Pauls, N. Röwert, M. Teroerde

RWTH Aachen University, III. Physikalisches Institut A, Aachen, Germany
S. Diekmann, A. Dodonova, N. Eich, D. Eliseev, F. Engelke, M. Erdmann, P. Fackeldey, B. Fischer, T. Hebbeker, K. Hoepfner, F. Ivone, A. Jung, M.y. Lee, L. Mastrolorenzo, M. Merschmeyer, A. Meyer, S. Mukherjee, D. Noll, A. Novak, F. Nowotny, A. Pozdnyakov, Y. Rath, W. Redjeb, F. Rehm, H. Reithler, V. Sarkisovi, A. Schmidt, S.C. Schuler, A. Sharma, A. Stein, F. Torres Da Silva De Araujo[19], L. Vigilante, S. Wiedenbeck, S. Zaleski

RWTH Aachen University, III. Physikalisches Institut B, Aachen, Germany
C. Dziwok, G. Flügge, W. Haj Ahmad[20], T. Kress, A. Nowack, O. Pooth, A. Stahl, T. Ziemons, A. Zotz

Deutsches Elektronen-Synchrotron, Hamburg, Germany
H. Aarup Petersen, M. Aldaya Martin, J. Alimena, S. Amoroso, Y. An, S. Baxter, M. Bayatmakou, H. Becerril Gonzalez, O. Behnke, A. Belvedere, S. Bhattacharya,

JHEP03(2024)134

F. Blekman[21], K. Borras[22], D. Brunner, A. Campbell, A. Cardini, C. Cheng, F. Colombina, S. Consuegra Rodríguez, G. Correia Silva, M. De Silva, G. Eckerlin, D. Eckstein, L.I. Estevez Banos, O. Filatov, E. Gallo[21], A. Geiser, A. Giraldi, G. Greau, V. Guglielmi, M. Guthoff, A. Hinzmann, A. Jafari[23], L. Jeppe, N.Z. Jomhari, B. Kaech, M. Kasemann, H. Kaveh, C. Kleinwort, R. Kogler, M. Komm, D. Krücker, W. Lange, D. Leyva Pernia, K. Lipka[24], W. Lohmann[25], R. Mankel, I.-A. Melzer-Pellmann, M. Mendizabal Morentin, J. Metwally, A.B. Meyer, G. Milella, A. Mussgiller, A. Nürnberg, Y. Otarid, D. Pérez Adán, E. Ranken, A. Raspereza, B. Ribeiro Lopes, J. Rübenach, A. Saggio, M. Scham[26,22], V. Scheurer, S. Schnake[22], P. Schütze, C. Schwanenberger[21], M. Shchedrolosiev, R.E. Sosa Ricardo, L.P. Sreelatha Pramod, D. Stafford, F. Vazzoler, A. Ventura Barroso, R. Walsh, Q. Wang, Y. Wen, K. Wichmann, L. Wiens[22], C. Wissing, S. Wuchterl, Y. Yang, A. Zimermmane Castro Santos

University of Hamburg, Hamburg, Germany

A. Albrecht, S. Albrecht, M. Antonello, S. Bein, L. Benato, M. Bonanomi, P. Connor, M. Eich, K. El Morabit, Y. Fischer, A. Fröhlich, C. Garbers, E. Garutti, A. Grohsjean, M. Hajheidari, J. Haller, H.R. Jabusch, G. Kasieczka, P. Keicher, R. Klanner, W. Korcari, T. Kramer, V. Kutzner, F. Labe, J. Lange, A. Lobanov, C. Matthies, A. Mehta, L. Moureaux, M. Mrowietz, A. Nigamova, Y. Nissan, A. Paasch, K.J. Pena Rodriguez, T. Quadfasel, B. Raciti, M. Rieger, D. Savoiu, J. Schindler, P. Schleper, M. Schröder, J. Schwandt, M. Sommerhalder, H. Stadie, G. Steinbrück, A. Tews, M. Wolf

Karlsruher Institut fuer Technologie, Karlsruhe, Germany

S. Brommer, M. Burkart, E. Butz, T. Chwalek, A. Dierlamm, A. Droll, N. Faltermann, M. Giffels, A. Gottmann, F. Hartmann[27], M. Horzela, U. Husemann, M. Klute, R. Koppenhöfer, M. Link, A. Lintuluoto, S. Maier, S. Mitra, M. Mormile, Th. Müller, M. Neukum, M. Oh, G. Quast, K. Rabbertz, I. Shvetsov, H.J. Simonis, N. Trevisani, R. Ulrich, J. van der Linden, R.F. Von Cube, M. Wassmer, S. Wieland, F. Wittig, R. Wolf, S. Wunsch, X. Zuo

Institute of Nuclear and Particle Physics (INPP), NCSR Demokritos, Aghia Paraskevi, Greece

G. Anagnostou, P. Assiouras, G. Daskalakis, A. Kyriakis, A. Papadopoulos[27], A. Stakia

National and Kapodistrian University of Athens, Athens, Greece

D. Karasavvas, P. Kontaxakis, G. Melachroinos, A. Panagiotou, I. Papavergou, I. Paraskevas, N. Saoulidou, K. Theofilatos, E. Tziaferi, K. Vellidis, I. Zisopoulos

National Technical University of Athens, Athens, Greece

G. Bakas, T. Chatzistavrou, G. Karapostoli, K. Kousouris, I. Papakrivopoulos, E. Siamarkou, G. Tsipolitis, A. Zacharopoulou

University of Ioánnina, Ioánnina, Greece

K. Adamidis, I. Bestintzanos, I. Evangelou, C. Foudas, P. Gianneios, C. Kamtsikis, P. Katsoulis, P. Kokkas, P.G. Kosmoglou Kioseoglou, N. Manthos, I. Papadopoulos, J. Strologas

HUN-REN Wigner Research Centre for Physics, Budapest, Hungary
M. Bartók[28], C. Hajdu, D. Horvath[29,30], F. Sikler, V. Veszpremi

MTA-ELTE Lendület CMS Particle and Nuclear Physics Group, Eötvös Loránd University, Budapest, Hungary
M. Csanád, K. Farkas, M.M.A. Gadallah[31], Á. Kadlecsik, P. Major, K. Mandal, G. Pásztor, A.J. Rádl[32], G.I. Veres

Faculty of Informatics, University of Debrecen, Debrecen, Hungary
P. Raics, B. Ujvari[33], G. Zilizi

Institute of Nuclear Research ATOMKI, Debrecen, Hungary
G. Bencze, S. Czellar, J. Karancsi[28], J. Molnar, Z. Szillasi

Karoly Robert Campus, MATE Institute of Technology, Gyongyos, Hungary
T. Csorgo[32], F. Nemes[32], T. Novak

Panjab University, Chandigarh, India
J. Babbar, S. Bansal, S.B. Beri, V. Bhatnagar, G. Chaudhary, S. Chauhan, N. Dhingra[34], R. Gupta, A. Kaur, A. Kaur, H. Kaur, M. Kaur, S. Kumar, P. Kumari, M. Meena, K. Sandeep, T. Sheokand, J.B. Singh[35], A. Singla

University of Delhi, Delhi, India
A. Ahmed, A. Bhardwaj, A. Chhetri, B.C. Choudhary, A. Kumar, M. Naimuddin, K. Ranjan, S. Saumya

Saha Institute of Nuclear Physics, HBNI, Kolkata, India
S. Baradia, S. Barman[36], S. Bhattacharya, D. Bhowmik, S. Dutta, S. Dutta, B. Gomber[37], P. Palit, G. Saha, B. Sahu[37], S. Sarkar

Indian Institute of Technology Madras, Madras, India
M.M. Ameen, P.K. Behera, S.C. Behera, S. Chatterjee, P. Jana, P. Kalbhor, J.R. Komaragiri[38], D. Kumar[38], L. Panwar[38], R. Pradhan, P.R. Pujahari, N.R. Saha, A. Sharma, A.K. Sikdar, S. Verma

Tata Institute of Fundamental Research-A, Mumbai, India
T. Aziz, I. Das, S. Dugad, M. Kumar, G.B. Mohanty, P. Suryadevara

Tata Institute of Fundamental Research-B, Mumbai, India
A. Bala, S. Banerjee, R.M. Chatterjee, M. Guchait, S. Karmakar, S. Kumar, G. Majumder, K. Mazumdar, S. Mukherjee, A. Thachayath

National Institute of Science Education and Research, An OCC of Homi Bhabha National Institute, Bhubaneswar, Odisha, India
S. Bahinipati[39], A.K. Das, C. Kar, D. Maity[40], P. Mal, T. Mishra, V.K. Muraleedharan Nair Bindhu[40], K. Naskar[40], A. Nayak[40], P. Sadangi, P. Saha, S.K. Swain, S. Varghese[40], D. Vats[40]

Indian Institute of Science Education and Research (IISER), Pune, India
A. Alpana, S. Dube, B. Kansal, A. Laha, A. Rastogi, S. Sharma

Isfahan University of Technology, Isfahan, Iran
H. Bakhshiansohi[41], E. Khazaie[42], M. Zeinali[43]

Institute for Research in Fundamental Sciences (IPM), Tehran, Iran
S. Chenarani[44], S.M. Etesami, M. Khakzad, M. Mohammadi Najafabadi

University College Dublin, Dublin, Ireland
M. Grunewald

INFN Sezione di Bari[a], Università di Bari[b], Politecnico di Bari[c], Bari, Italy
M. Abbrescia[a,b], R. Aly[a,c,45], A. Colaleo[a,b], D. Creanza[a,c], B. D'Anzi[a,b], N. De Filippis[a,c], M. De Palma[a,b], A. Di Florio[a,c], W. Elmetenawee[a,b,45], L. Fiore[a], G. Iaselli[a,c], G. Maggi[a,c], M. Maggi[a], I. Margjeka[a,b], V. Mastrapasqua[a,b], S. My[a,b], S. Nuzzo[a,b], A. Pellecchia[a,b], A. Pompili[a,b], G. Pugliese[a,c], R. Radogna[a], G. Ramirez-Sanchez[a,c], D. Ramos[a], A. Ranieri[a], L. Silvestris[a], F.M. Simone[a,b], Ü. Sözbilir[a], A. Stamerra[a], R. Venditti[a], P. Verwilligen[a], A. Zaza[a,b]

INFN Sezione di Bologna[a], Università di Bologna[b], Bologna, Italy
G. Abbiendi[a], C. Battilana[a,b], D. Bonacorsi[a,b], L. Borgonovi[a], P. Capiluppi[a,b], A. Castro[a,b], F.R. Cavallo[a], M. Cuffiani[a,b], G.M. Dallavalle[a], T. Diotalevi[a,b], F. Fabbri[a], A. Fanfani[a,b], D. Fasanella[a,b], P. Giacomelli[a], L. Giommi[a,b], C. Grandi[a], L. Guiducci[a,b], S. Lo Meo[a,46], L. Lunerti[a,b], S. Marcellini[a], G. Masetti[a], F.L. Navarria[a,b], A. Perrotta[a], F. Primavera[a,b], A.M. Rossi[a,b], T. Rovelli[a,b], G.P. Siroli[a,b]

INFN Sezione di Catania[a], Università di Catania[b], Catania, Italy
S. Costa[a,b,47], A. Di Mattia[a], R. Potenza[a,b], A. Tricomi[a,b,47], C. Tuve[a,b]

INFN Sezione di Firenze[a], Università di Firenze[b], Firenze, Italy
G. Barbagli[a], G. Bardelli[a,b], B. Camaiani[a,b], A. Cassese[a], R. Ceccarelli[a], V. Ciulli[a,b], C. Civinini[a], R. D'Alessandro[a,b], E. Focardi[a,b], G. Latino[a,b], P. Lenzi[a,b], M. Lizzo[a,b], M. Meschini[a], S. Paoletti[a], A. Papanastassiou[a,b], G. Sguazzoni[a], L. Viliani[a]

INFN Laboratori Nazionali di Frascati, Frascati, Italy
L. Benussi, S. Bianco, S. Meola[48], D. Piccolo

INFN Sezione di Genova[a], Università di Genova[b], Genova, Italy
P. Chatagnon[a], F. Ferro[a], E. Robutti[a], S. Tosi[a,b]

INFN Sezione di Milano-Bicocca[a], Università di Milano-Bicocca[b], Milano, Italy
A. Benaglia[a], G. Boldrini[a], F. Brivio[a], F. Cetorelli[a], F. De Guio[a,b], M.E. Dinardo[a,b], P. Dini[a], S. Gennai[a], A. Ghezzi[a,b], P. Govoni[a,b], L. Guzzi[a], M.T. Lucchini[a,b], M. Malberti[a], S. Malvezzi[a], A. Massironi[a], D. Menasce[a], L. Moroni[a], M. Paganoni[a,b], D. Pedrini[a], B.S. Pinolini[a], S. Ragazzi[a,b], N. Redaelli[a], T. Tabarelli de Fatis[a,b], D. Zuolo[a]

JHEP03(2024)134

INFN Sezione di Napoli[a], Università di Napoli 'Federico II'[b], Napoli, Italy; Università della Basilicata[c], Potenza, Italy; Università G. Marconi[d], Roma, Italy

S. Buontempo[a], A. Cagnotta[a,b], F. Carnevali[a,b], N. Cavallo[a,c], A. De Iorio[a,b], F. Fabozzi[a,c], A.O.M. Iorio[a,b], L. Lista[a,b,49], P. Paolucci[a,27], B. Rossi[a], C. Sciacca[a,b]

INFN Sezione di Padova[a], Università di Padova[b], Padova, Italy; Università di Trento[c], Trento, Italy

R. Ardino[a], P. Azzi[a], N. Bacchetta[a,50], M. Bellato[a], D. Bisello[a,b], P. Bortignon[a], A. Bragagnolo[a,b], R. Carlin[a,b], P. Checchia[a], T. Dorigo[a], F. Gasparini[a,b], U. Gasparini[a,b], G. Grosso[a], L. Layer[a,51], E. Lusiani[a], M. Margoni[a,b], A.T. Meneguzzo[a,b], M. Migliorini[a,b], J. Pazzini[a,b], P. Ronchese[a,b], R. Rossin[a,b], G. Strong[a], M. Tosi[a,b], A. Triossi[a,b], S. Ventura[a], H. Yarar[a,b], M. Zanetti[a,b], P. Zotto[a,b], A. Zucchetta[a,b], G. Zumerle[a,b]

INFN Sezione di Pavia[a], Università di Pavia[b], Pavia, Italy

S. Abu Zeid[a,52], C. Aimè[a,b], A. Braghieri[a], S. Calzaferri[a,b], D. Fiorina[a,b], P. Montagna[a,b], V. Re[a], C. Riccardi[a,b], P. Salvini[a], I. Vai[a,b], P. Vitulo[a,b]

INFN Sezione di Perugia[a], Università di Perugia[b], Perugia, Italy

S. Ajmal[a,b], P. Asenov[a,53], G.M. Bilei[a], D. Ciangottini[a,b], L. Fanò[a,b], M. Magherini[a,b], G. Mantovani[a,b], V. Mariani[a,b], M. Menichelli[a], F. Moscatelli[a,53], A. Piccinelli[a,b], M. Presilla[a,b], A. Rossi[a,b], A. Santocchia[a,b], D. Spiga[a], T. Tedeschi[a,b]

INFN Sezione di Pisa[a], Università di Pisa[b], Scuola Normale Superiore di Pisa[c], Pisa, Italy; Università di Siena[d], Siena, Italy

P. Azzurri[a], G. Bagliesi[a], R. Bhattacharya[a], L. Bianchini[a,b], T. Boccali[a], E. Bossini[a], D. Bruschini[a,c], R. Castaldi[a], M.A. Ciocci[a,b], M. Cipriani[a,b], V. D'Amante[a,d], R. Dell'Orso[a], S. Donato[a], A. Giassi[a], F. Ligabue[a,c], D. Matos Figueiredo[a], A. Messineo[a,b], M. Musich[a,b], F. Palla[a], S. Parolia[a], A. Rizzi[a,b], G. Rolandi[a,c], S. Roy Chowdhury[a], T. Sarkar[a], A. Scribano[a], P. Spagnolo[a], R. Tenchini[a,b], G. Tonelli[a,b], N. Turini[a,d], A. Venturi[a], P.G. Verdini[a]

INFN Sezione di Roma[a], Sapienza Università di Roma[b], Roma, Italy

P. Barria[a], M. Campana[a,b], F. Cavallari[a], L. Cunqueiro Mendez[a,b], D. Del Re[a,b], E. Di Marco[a], M. Diemoz[a], F. Errico[a,b], E. Longo[a,b], P. Meridiani[a], J. Mijuskovic[a,b], G. Organtini[a,b], F. Pandolfi[a], R. Paramatti[a,b], C. Quaranta[a,b], S. Rahatlou[a,b], C. Rovelli[a], F. Santanastasio[a,b], L. Soffi[a], R. Tramontano[a,b]

INFN Sezione di Torino[a], Università di Torino[b], Torino, Italy; Università del Piemonte Orientale[c], Novara, Italy

N. Amapane[a,b], R. Arcidiacono[a,c], S. Argiro[a,b], M. Arneodo[a,c], N. Bartosik[a], R. Bellan[a,b], A. Bellora[a,b], C. Biino[a], N. Cartiglia[a], M. Costa[a,b], R. Covarelli[a,b], N. Demaria[a], L. Finco[a], M. Grippo[a,b], B. Kiani[a,b], F. Legger[a], F. Luongo[a,b], C. Mariotti[a], S. Maselli[a], A. Mecca[a,b], E. Migliore[a,b], M. Monteno[a], R. Mulargia[a], M.M. Obertino[a,b], G. Ortona[a], L. Pacher[a,b], N. Pastrone[a], M. Pelliccioni[a], M. Ruspa[a,c],

F. Siviero[a,b], V. Sola[a,b], A. Solano[a,b], D. Soldi[a,b], A. Staiano[a], C. Tarricone[a,b], M. Tornago[a,b], D. Trocino[a], G. Umoret[a,b], E. Vlasov[a,b]

INFN Sezione di Trieste[a], Università di Trieste[b], Trieste, Italy
S. Belforte[a], V. Candelise[a,b], M. Casarsa[a], F. Cossutti[a], K. De Leo[a,b], G. Della Ricca[a,b]

Kyungpook National University, Daegu, Korea
S. Dogra, J. Hong, C. Huh, B. Kim, D.H. Kim, J. Kim, H. Lee, S.W. Lee, C.S. Moon, Y.D. Oh, S.I. Pak, M.S. Ryu, S. Sekmen, Y.C. Yang

Chonnam National University, Institute for Universe and Elementary Particles, Kwangju, Korea
G. Bak, P. Gwak, H. Kim, D.H. Moon

Hanyang University, Seoul, Korea
E. Asilar, D. Kim, T.J. Kim, J.A. Merlin, J. Park

Korea University, Seoul, Korea
S. Choi, S. Han, B. Hong, K. Lee, K.S. Lee, J. Park, S.K. Park, J. Yoo

Kyung Hee University, Department of Physics, Seoul, Korea
J. Goh

Sejong University, Seoul, Korea
H. S. Kim, Y. Kim, S. Lee

Seoul National University, Seoul, Korea
J. Almond, J.H. Bhyun, J. Choi, S. Jeon, W. Jun, J. Kim, J.S. Kim, S. Ko, H. Kwon, H. Lee, J. Lee, J. Lee, S. Lee, B.H. Oh, S.B. Oh, H. Seo, U.K. Yang, I. Yoon

University of Seoul, Seoul, Korea
W. Jang, D.Y. Kang, Y. Kang, S. Kim, B. Ko, J.S.H. Lee, Y. Lee, I.C. Park, Y. Roh, I.J. Watson, S. Yang

Yonsei University, Department of Physics, Seoul, Korea
S. Ha, H.D. Yoo

Sungkyunkwan University, Suwon, Korea
M. Choi, M.R. Kim, H. Lee, Y. Lee, I. Yu

College of Engineering and Technology, American University of the Middle East (AUM), Dasman, Kuwait
T. Beyrouthy, Y. Maghrbi

Riga Technical University, Riga, Latvia
K. Dreimanis, A. Gaile, G. Pikurs, A. Potrebko, M. Seidel, V. Veckalns[54]

JHEP03(2024)134

University of Latvia (LU), Riga, Latvia
N.R. Strautnieks

Vilnius University, Vilnius, Lithuania
M. Ambrozas, A. Juodagalvis, A. Rinkevicius, G. Tamulaitis

National Centre for Particle Physics, Universiti Malaya, Kuala Lumpur, Malaysia
N. Bin Norjoharuddeen, I. Yusuff[55], Z. Zolkapli

Universidad de Sonora (UNISON), Hermosillo, Mexico
J.F. Benitez, A. Castaneda Hernandez, H.A. Encinas Acosta, L.G. Gallegos Maríñez, M. León Coello, J.A. Murillo Quijada, A. Sehrawat, L. Valencia Palomo

Centro de Investigacion y de Estudios Avanzados del IPN, Mexico City, Mexico
G. Ayala, H. Castilla-Valdez, E. De La Cruz-Burelo, I. Heredia-De La Cruz[56], R. Lopez-Fernandez, C.A. Mondragon Herrera, A. Sánchez Hernández

Universidad Iberoamericana, Mexico City, Mexico
C. Oropeza Barrera, M. Ramírez García

Benemerita Universidad Autonoma de Puebla, Puebla, Mexico
I. Bautista, I. Pedraza, H.A. Salazar Ibarguen, C. Uribe Estrada

University of Montenegro, Podgorica, Montenegro
I. Bubanja, N. Raicevic

University of Canterbury, Christchurch, New Zealand
P.H. Butler

National Centre for Physics, Quaid-I-Azam University, Islamabad, Pakistan
A. Ahmad, M.I. Asghar, A. Awais, M.I.M. Awan, H.R. Hoorani, W.A. Khan

AGH University of Krakow, Faculty of Computer Science, Electronics and Telecommunications, Krakow, Poland
V. Avati, L. Grzanka, M. Malawski

National Centre for Nuclear Research, Swierk, Poland
H. Bialkowska, M. Bluj, B. Boimska, M. Górski, M. Kazana, M. Szleper, P. Zalewski

Institute of Experimental Physics, Faculty of Physics, University of Warsaw, Warsaw, Poland
K. Bunkowski, K. Doroba, A. Kalinowski, M. Konecki, J. Krolikowski, A. Muhammad

Warsaw University of Technology, Warsaw, Poland
K. Pozniak, W. Zabolotny

JHEP03(2024)134

Laboratório de Instrumentação e Física Experimental de Partículas, Lisboa, Portugal
M. Araujo, D. Bastos, C. Beirão Da Cruz E Silva, A. Boletti, M. Bozzo, P. Faccioli, M. Gallinaro, J. Hollar, N. Leonardo, T. Niknejad, A. Petrilli, M. Pisano, J. Seixas, J. Varela

Faculty of Physics, University of Belgrade, Belgrade, Serbia
P. Adzic, P. Milenovic

VINCA Institute of Nuclear Sciences, University of Belgrade, Belgrade, Serbia
M. Dordevic, J. Milosevic, V. Rekovic

Centro de Investigaciones Energéticas Medioambientales y Tecnológicas (CIEMAT), Madrid, Spain
M. Aguilar-Benitez, J. Alcaraz Maestre, M. Barrio Luna, Cristina F. Bedoya, M. Cepeda, M. Cerrada, N. Colino, B. De La Cruz, A. Delgado Peris, D. Fernández Del Val, J.P. Fernández Ramos, J. Flix, M.C. Fouz, O. Gonzalez Lopez, S. Goy Lopez, J.M. Hernandez, M.I. Josa, J. León Holgado, D. Moran, C. M. Morcillo Perez, Á. Navarro Tobar, C. Perez Dengra, A. Pérez-Calero Yzquierdo, J. Puerta Pelayo, I. Redondo, D.D. Redondo Ferrero, L. Romero, S. Sánchez Navas, L. Urda Gómez, J. Vazquez Escobar, C. Willmott

Universidad Autónoma de Madrid, Madrid, Spain
J.F. de Trocóniz

Universidad de Oviedo, Instituto Universitario de Ciencias y Tecnologías Espaciales de Asturias (ICTEA), Oviedo, Spain
B. Alvarez Gonzalez, J. Cuevas, J. Fernandez Menendez, S. Folgueras, I. Gonzalez Caballero, J.R. González Fernández, E. Palencia Cortezon, C. Ramón Álvarez, V. Rodríguez Bouza, A. Soto Rodríguez, A. Trapote, C. Vico Villalba, P. Vischia

Instituto de Física de Cantabria (IFCA), CSIC-Universidad de Cantabria, Santander, Spain
S. Bhowmik, S. Blanco Fernández, J.A. Brochero Cifuentes, I.J. Cabrillo, A. Calderon, J. Duarte Campderros, M. Fernandez, C. Fernandez Madrazo, G. Gomez, C. Lasaosa García, C. Martinez Rivero, P. Martinez Ruiz del Arbol, F. Matorras, P. Matorras Cuevas, E. Navarrete Ramos, J. Piedra Gomez, C. Prieels, L. Scodellaro, I. Vila, J.M. Vizan Garcia

University of Colombo, Colombo, Sri Lanka
M.K. Jayananda, B. Kailasapathy[57], D.U.J. Sonnadara, D.D.C. Wickramarathna

University of Ruhuna, Department of Physics, Matara, Sri Lanka
W.G.D. Dharmaratna[58], K. Liyanage, N. Perera, N. Wickramage

JHEP03(2024)134

CERN, European Organization for Nuclear Research, Geneva, Switzerland
D. Abbaneo, C. Amendola, E. Auffray, G. Auzinger, J. Baechler, D. Barney, A. Bermúdez Martínez, M. Bianco, B. Bilin, A.A. Bin Anuar, A. Bocci, E. Brondolin, C. Caillol, T. Camporesi, G. Cerminara, N. Chernyavskaya, D. d'Enterria, A. Dabrowski, A. David, A. De Roeck, M.M. Defranchis, M. Deile, M. Dobson, F. Fallavollita[59], L. Forthomme, G. Franzoni, W. Funk, S. Giani, D. Gigi, K. Gill, F. Glege, L. Gouskos, M. Haranko, J. Hegeman, V. Innocente, T. James, P. Janot, J. Kieseler, S. Laurila, P. Lecoq, E. Leutgeb, C. Lourenço, B. Maier, L. Malgeri, M. Mannelli, A.C. Marini, F. Meijers, S. Mersi, E. Meschi, V. Milosevic, F. Moortgat, M. Mulders, S. Orfanelli, F. Pantaleo, M. Peruzzi, G. Petrucciani, A. Pfeiffer, M. Pierini, D. Piparo, H. Qu, D. Rabady, G. Reales Gutiérrez, M. Rovere, H. Sakulin, S. Scarfi, M. Selvaggi, A. Sharma, K. Shchelina, P. Silva, P. Sphicas[60], A.G. Stahl Leiton, A. Steen, S. Summers, D. Treille, P. Tropea, A. Tsirou, D. Walter, J. Wanczyk[61], K.A. Wozniak[62], P. Zehetner, P. Zejdl, W.D. Zeuner

Paul Scherrer Institut, Villigen, Switzerland
T. Bevilacqua[63], L. Caminada[63], A. Ebrahimi, W. Erdmann, R. Horisberger, Q. Ingram, H.C. Kaestli, D. Kotlinski, C. Lange, M. Missiroli[63], L. Noehte[63], T. Rohe

ETH Zurich - Institute for Particle Physics and Astrophysics (IPA), Zurich, Switzerland
T.K. Aarrestad, K. Androsov[61], M. Backhaus, A. Calandri, C. Cazzaniga, K. Datta, A. De Cosa, G. Dissertori, M. Dittmar, M. Donegà, F. Eble, M. Galli, K. Gedia, F. Glessgen, C. Grab, D. Hits, W. Lustermann, A.-M. Lyon, R.A. Manzoni, M. Marchegiani, L. Marchese, C. Martin Perez, A. Mascellani[61], F. Nessi-Tedaldi, F. Pauss, V. Perovic, S. Pigazzini, M.G. Ratti, M. Reichmann, C. Reissel, T. Reitenspiess, B. Ristic, F. Riti, D. Ruini, D.A. Sanz Becerra, R. Seidita, J. Steggemann[61], D. Valsecchi, R. Wallny

Universität Zürich, Zurich, Switzerland
C. Amsler[64], P. Bärtschi, C. Botta, D. Brzhechko, M.F. Canelli, K. Cormier, R. Del Burgo, J.K. Heikkilä, M. Huwiler, W. Jin, A. Jofrehei, B. Kilminster, S. Leontsinis, S.P. Liechti, A. Macchiolo, P. Meiring, V.M. Mikuni, U. Molinatti, I. Neutelings, A. Reimers, P. Robmann, S. Sanchez Cruz, K. Schweiger, M. Senger, Y. Takahashi

National Central University, Chung-Li, Taiwan
C. Adloff[65], C.M. Kuo, W. Lin, P.K. Rout, P.C. Tiwari[38], S.S. Yu

National Taiwan University (NTU), Taipei, Taiwan
L. Ceard, Y. Chao, K.F. Chen, P.s. Chen, Z.g. Chen, W.-S. Hou, T.h. Hsu, Y.w. Kao, R. Khurana, G. Kole, Y.y. Li, R.-S. Lu, E. Paganis, A. Psallidas, X.f. Su, J. Thomas-Wilsker, H.y. Wu, E. Yazgan

High Energy Physics Research Unit, Department of Physics, Faculty of Science, Chulalongkorn University, Bangkok, Thailand
C. Asawatangtrakuldee, N. Srimanobhas, V. Wachirapusitanand

Çukurova University, Physics Department, Science and Art Faculty, Adana, Turkey
D. Agyel, F. Boran, Z.S. Demiroglu, F. Dolek, I. Dumanoglu[66], E. Eskut, Y. Guler[67], E. Gurpinar Guler[67], C. Isik, O. Kara, A. Kayis Topaksu, U. Kiminsu, G. Onengut, K. Ozdemir[68], A. Polatoz, B. Tali[69], U.G. Tok, S. Turkcapar, E. Uslan, I.S. Zorbakir

Middle East Technical University, Physics Department, Ankara, Turkey
K. Ocalan[70], M. Yalvac[71]

Bogazici University, Istanbul, Turkey
B. Akgun, I.O. Atakisi, E. Gülmez, M. Kaya[72], O. Kaya[73], S. Tekten[74]

Istanbul Technical University, Istanbul, Turkey
A. Cakir, K. Cankocak[66], Y. Komurcu, S. Sen[75]

Istanbul University, Istanbul, Turkey
O. Aydilek, S. Cerci[69], V. Epshteyn, B. Hacisahinoglu, I. Hos[76], B. Isildak[77], B. Kaynak, S. Ozkorucuklu, O. Potok, H. Sert, C. Simsek, D. Sunar Cerci[69], C. Zorbilmez

Institute for Scintillation Materials of National Academy of Science of Ukraine, Kharkiv, Ukraine
A. Boyaryntsev, B. Grynyov

National Science Centre, Kharkiv Institute of Physics and Technology, Kharkiv, Ukraine
L. Levchuk

University of Bristol, Bristol, United Kingdom
D. Anthony, J.J. Brooke, A. Bundock, F. Bury, E. Clement, D. Cussans, H. Flacher, M. Glowacki, J. Goldstein, H.F. Heath, L. Kreczko, B. Krikler, S. Paramesvaran, S. Seif El Nasr-Storey, V.J. Smith, N. Stylianou[78], K. Walkingshaw Pass, R. White

Rutherford Appleton Laboratory, Didcot, United Kingdom
A.H. Ball, K.W. Bell, A. Belyaev[79], C. Brew, R.M. Brown, D.J.A. Cockerill, C. Cooke, K.V. Ellis, K. Harder, S. Harper, M.-L. Holmberg[80], Sh. Jain, J. Linacre, K. Manolopoulos, D.M. Newbold, E. Olaiya, D. Petyt, T. Reis, G. Salvi, T. Schuh, C.H. Shepherd-Themistocleous, I.R. Tomalin, T. Williams

Imperial College, London, United Kingdom
R. Bainbridge, P. Bloch, C.E. Brown, O. Buchmuller, V. Cacchio, C.A. Carrillo Montoya, G.S. Chahal[81], D. Colling, J.S. Dancu, P. Dauncey, G. Davies, J. Davies, M. Della Negra, S. Fayer, G. Fedi, G. Hall, M.H. Hassanshahi, A. Howard, G. Iles, M. Knight, J. Langford, L. Lyons, A.-M. Magnan, S. Malik, A. Martelli, M. Mieskolainen, J. Nash[82], M. Pesaresi, B.C. Radburn-Smith, A. Richards, A. Rose, C. Seez, R. Shukla,

JHEP03(2024)134

A. Tapper, K. Uchida, G.P. Uttley, L.H. Vage, T. Virdee[27], M. Vojinovic, N. Wardle, D. Winterbottom

Brunel University, Uxbridge, United Kingdom
K. Coldham, J.E. Cole, A. Khan, P. Kyberd, I.D. Reid

Baylor University, Waco, Texas, USA
S. Abdullin, A. Brinkerhoff, B. Caraway, J. Dittmann, K. Hatakeyama, J. Hiltbrand, A.R. Kanuganti, B. McMaster, M. Saunders, S. Sawant, C. Sutantawibul, M. Toms[83], J. Wilson

Catholic University of America, Washington, DC, USA
R. Bartek, A. Dominguez, C. Huerta Escamilla, A.E. Simsek, R. Uniyal, A.M. Vargas Hernandez

The University of Alabama, Tuscaloosa, Alabama, USA
R. Chudasama, S.I. Cooper, S.V. Gleyzer, C.U. Perez, P. Rumerio[84], E. Usai, C. West, R. Yi

Boston University, Boston, Massachusetts, USA
A. Akpinar, A. Albert, D. Arcaro, C. Cosby, Z. Demiragli, C. Erice, E. Fontanesi, D. Gastler, J. Rohlf, K. Salyer, D. Sperka, D. Spitzbart, I. Suarez, A. Tsatsos, S. Yuan

Brown University, Providence, Rhode Island, USA
G. Benelli, X. Coubez[22], D. Cutts, M. Hadley, U. Heintz, J.M. Hogan[85], T. Kwon, G. Landsberg, K.T. Lau, D. Li, J. Luo, S. Mondal, M. Narain[†], N. Pervan, S. Sagir[86], F. Simpson, M. Stamenkovic, W.Y. Wong, X. Yan, W. Zhang

University of California, Davis, Davis, California, USA
S. Abbott, J. Bonilla, C. Brainerd, R. Breedon, M. Calderon De La Barca Sanchez, M. Chertok, M. Citron, J. Conway, P.T. Cox, R. Erbacher, G. Haza, F. Jensen, O. Kukral, G. Mocellin, M. Mulhearn, D. Pellett, B. Regnery, W. Wei, Y. Yao, F. Zhang

University of California, Los Angeles, California, USA
M. Bachtis, R. Cousins, A. Datta, J. Hauser, M. Ignatenko, M.A. Iqbal, T. Lam, E. Manca, W.A. Nash, D. Saltzberg, B. Stone, V. Valuev

University of California, Riverside, Riverside, California, USA
R. Clare, M. Gordon, G. Hanson, W. Si, S. Wimpenny[†]

University of California, San Diego, La Jolla, California, USA
J.G. Branson, S. Cittolin, S. Cooperstein, D. Diaz, J. Duarte, R. Gerosa, L. Giannini, J. Guiang, R. Kansal, V. Krutelyov, R. Lee, J. Letts, M. Masciovecchio, F. Mokhtar,

M. Pieri, M. Quinnan, B.V. Sathia Narayanan, V. Sharma, M. Tadel, E. Vourliotis, F. Würthwein, Y. Xiang, A. Yagil

University of California, Santa Barbara - Department of Physics, Santa Barbara, California, USA

A. Barzdukas, L. Brennan, C. Campagnari, G. Collura, A. Dorsett, J. Incandela, M. Kilpatrick, J. Kim, A.J. Li, P. Masterson, H. Mei, M. Oshiro, J. Richman, U. Sarica, R. Schmitz, F. Setti, J. Sheplock, D. Stuart, S. Wang

California Institute of Technology, Pasadena, California, USA

A. Bornheim, O. Cerri, A. Latorre, J.M. Lawhorn, J. Mao, H.B. Newman, T. Q. Nguyen, M. Spiropulu, J.R. Vlimant, C. Wang, S. Xie, R.Y. Zhu

Carnegie Mellon University, Pittsburgh, Pennsylvania, USA

J. Alison, S. An, M.B. Andrews, P. Bryant, V. Dutta, T. Ferguson, A. Harilal, C. Liu, T. Mudholkar, S. Murthy, M. Paulini, A. Roberts, A. Sanchez, W. Terrill

University of Colorado Boulder, Boulder, Colorado, USA

J.P. Cumalat, W.T. Ford, A. Hassani, G. Karathanasis, E. MacDonald, N. Manganelli, F. Marini, A. Perloff, C. Savard, N. Schonbeck, K. Stenson, K.A. Ulmer, S.R. Wagner, N. Zipper

Cornell University, Ithaca, New York, USA

J. Alexander, S. Bright-Thonney, X. Chen, D.J. Cranshaw, J. Fan, X. Fan, D. Gadkari, S. Hogan, J. Monroy, J.R. Patterson, J. Reichert, M. Reid, A. Ryd, J. Thom, P. Wittich, R. Zou

Fermi National Accelerator Laboratory, Batavia, Illinois, USA

M. Albrow, M. Alyari, O. Amram, G. Apollinari, A. Apresyan, L.A.T. Bauerdick, D. Berry, J. Berryhill, P.C. Bhat, K. Burkett, J.N. Butler, A. Canepa, G.B. Cerati, H.W.K. Cheung, F. Chlebana, G. Cummings, J. Dickinson, I. Dutta, V.D. Elvira, Y. Feng, J. Freeman, A. Gandrakota, Z. Gecse, L. Gray, D. Green, S. Grünendahl, D. Guerrero, O. Gutsche, R.M. Harris, R. Heller, T.C. Herwig, J. Hirschauer, L. Horyn, B. Jayatilaka, S. Jindariani, M. Johnson, U. Joshi, T. Klijnsma, B. Klima, K.H.M. Kwok, S. Lammel, D. Lincoln, R. Lipton, T. Liu, C. Madrid, K. Maeshima, C. Mantilla, D. Mason, P. McBride, P. Merkel, S. Mrenna, S. Nahn, J. Ngadiuba, D. Noonan, V. Papadimitriou, N. Pastika, K. Pedro, C. Pena[87], F. Ravera, A. Reinsvold Hall[88], L. Ristori, E. Sexton-Kennedy, N. Smith, A. Soha, L. Spiegel, S. Stoynev, L. Taylor, S. Tkaczyk, N.V. Tran, L. Uplegger, E.W. Vaandering, I. Zoi

University of Florida, Gainesville, Florida, USA

C. Aruta, P. Avery, D. Bourilkov, L. Cadamuro, P. Chang, V. Cherepanov, R.D. Field, E. Koenig, M. Kolosova, J. Konigsberg, A. Korytov, K.H. Lo, K. Matchev, N. Menendez, G. Mitselmakher, A. Muthirakalayil Madhu, N. Rawal, D. Rosenzweig, S. Rosenzweig, K. Shi, J. Wang

Florida State University, Tallahassee, Florida, USA
T. Adams, A. Al Kadhim, A. Askew, N. Bower, R. Habibullah, V. Hagopian, R. Hashmi, R.S. Kim, S. Kim, T. Kolberg, G. Martinez, H. Prosper, P.R. Prova, O. Viazlo, M. Wulansatiti, R. Yohay, J. Zhang

Florida Institute of Technology, Melbourne, Florida, USA
B. Alsufyani, M.M. Baarmand, S. Butalla, T. Elkafrawy[52], M. Hohlmann, R. Kumar Verma, M. Rahmani

University of Illinois Chicago, Chicago, USA, Chicago, USA
M.R. Adams, C. Bennett, R. Cavanaugh, S. Dittmer, R. Escobar Franco, O. Evdokimov, C.E. Gerber, D.J. Hofman, J.h. Lee, D. S. Lemos, A.H. Merrit, C. Mills, S. Nanda, G. Oh, B. Ozek, D. Pilipovic, T. Roy, S. Rudrabhatla, M.B. Tonjes, N. Varelas, X. Wang, Z. Ye, J. Yoo

The University of Iowa, Iowa City, Iowa, USA
M. Alhusseini, D. Blend, K. Dilsiz[89], L. Emediato, G. Karaman, O.K. Köseyan, J.-P. Merlo, A. Mestvirishvili[90], J. Nachtman, O. Neogi, H. Ogul[91], Y. Onel, A. Penzo, C. Snyder, E. Tiras[92]

Johns Hopkins University, Baltimore, Maryland, USA
B. Blumenfeld, L. Corcodilos, J. Davis, A.V. Gritsan, L. Kang, S. Kyriacou, P. Maksimovic, M. Roguljic, J. Roskes, S. Sekhar, M. Swartz, T.Á. Vámi

The University of Kansas, Lawrence, Kansas, USA
A. Abreu, L.F. Alcerro Alcerro, J. Anguiano, P. Baringer, A. Bean, Z. Flowers, D. Grove, J. King, G. Krintiras, M. Lazarovits, C. Le Mahieu, C. Lindsey, J. Marquez, N. Minafra, M. Murray, M. Nickel, M. Pitt, S. Popescu[93], C. Rogan, C. Royon, R. Salvatico, S. Sanders, C. Smith, Q. Wang, G. Wilson

Kansas State University, Manhattan, Kansas, USA
B. Allmond, A. Ivanov, K. Kaadze, A. Kalogeropoulos, D. Kim, Y. Maravin, K. Nam, J. Natoli, D. Roy, G. Sorrentino

Lawrence Livermore National Laboratory, Livermore, California, USA
F. Rebassoo, D. Wright

University of Maryland, College Park, Maryland, USA
E. Adams, A. Baden, O. Baron, A. Belloni, A. Bethani, Y.M. Chen, S.C. Eno, N.J. Hadley, S. Jabeen, R.G. Kellogg, T. Koeth, Y. Lai, S. Lascio, A.C. Mignerey, S. Nabili, C. Palmer, C. Papageorgakis, M.M. Paranjpe, L. Wang, K. Wong

Massachusetts Institute of Technology, Cambridge, Massachusetts, USA
J. Bendavid, W. Busza, I.A. Cali, Y. Chen, M. D'Alfonso, J. Eysermans, C. Freer, G. Gomez-Ceballos, M. Goncharov, P. Harris, D. Hoang, D. Kovalskyi, J. Krupa, L. Lavezzo,

JHEP03(2024)134

Y.-J. Lee, K. Long, C. Mironov, C. Paus, D. Rankin, C. Roland, G. Roland, S. Rothman, Z. Shi, G.S.F. Stephans, J. Wang, Z. Wang, B. Wyslouch, T. J. Yang

University of Minnesota, Minneapolis, Minnesota, USA
B. Crossman, B.M. Joshi, C. Kapsiak, M. Krohn, D. Mahon, J. Mans, B. Marzocchi, S. Pandey, M. Revering, R. Rusack, R. Saradhy, N. Schroeder, N. Strobbe, M.A. Wadud

University of Mississippi, Oxford, Mississippi, USA
L.M. Cremaldi

University of Nebraska-Lincoln, Lincoln, Nebraska, USA
K. Bloom, M. Bryson, D.R. Claes, C. Fangmeier, F. Golf, J. Hossain, C. Joo, I. Kravchenko, I. Reed, J.E. Siado, G.R. Snow†, W. Tabb, A. Vagnerini, A. Wightman, F. Yan, D. Yu, A.G. Zecchinelli

State University of New York at Buffalo, Buffalo, New York, USA
G. Agarwal, H. Bandyopadhyay, L. Hay, I. Iashvili, A. Kharchilava, C. McLean, M. Morris, D. Nguyen, J. Pekkanen, S. Rappoccio, H. Rejeb Sfar, A. Williams

Northeastern University, Boston, Massachusetts, USA
G. Alverson, E. Barberis, Y. Haddad, Y. Han, A. Krishna, J. Li, M. Lu, G. Madigan, D.M. Morse, V. Nguyen, T. Orimoto, A. Parker, L. Skinnari, A. Tishelman-Charny, B. Wang, D. Wood

Northwestern University, Evanston, Illinois, USA
S. Bhattacharya, J. Bueghly, Z. Chen, K.A. Hahn, Y. Liu, Y. Miao, D.G. Monk, M.H. Schmitt, A. Taliercio, M. Velasco

University of Notre Dame, Notre Dame, Indiana, USA
R. Band, R. Bucci, S. Castells, M. Cremonesi, A. Das, R. Goldouzian, M. Hildreth, K.W. Ho, K. Hurtado Anampa, C. Jessop, K. Lannon, J. Lawrence, N. Loukas, L. Lutton, J. Mariano, N. Marinelli, I. Mcalister, T. McCauley, C. Mcgrady, K. Mohrman, C. Moore, Y. Musienko[12], H. Nelson, M. Osherson, R. Ruchti, A. Townsend, M. Wayne, H. Yockey, M. Zarucki, L. Zygala

The Ohio State University, Columbus, Ohio, USA
A. Basnet, B. Bylsma, M. Carrigan, L.S. Durkin, C. Hill, M. Joyce, A. Lesauvage, M. Nunez Ornelas, K. Wei, B.L. Winer, B. R. Yates

Princeton University, Princeton, New Jersey, USA
F.M. Addesa, H. Bouchamaoui, P. Das, G. Dezoort, P. Elmer, A. Frankenthal, B. Greenberg, N. Haubrich, S. Higginbotham, G. Kopp, S. Kwan, D. Lange, A. Loeliger, D. Marlow, I. Ojalvo, J. Olsen, D. Stickland, C. Tully

University of Puerto Rico, Mayaguez, Puerto Rico, USA
S. Malik

Purdue University, West Lafayette, Indiana, USA
A.S. Bakshi, V.E. Barnes, S. Chandra, R. Chawla, S. Das, A. Gu, L. Gutay, M. Jones, A.W. Jung, D. Kondratyev, A.M. Koshy, M. Liu, G. Negro, N. Neumeister, G. Paspalaki, S. Piperov, A. Purohit, J.F. Schulte, M. Stojanovic, J. Thieman, A. K. Virdi, F. Wang, W. Xie

Purdue University Northwest, Hammond, Indiana, USA
J. Dolen, N. Parashar, A. Pathak

Rice University, Houston, Texas, USA
D. Acosta, A. Baty, T. Carnahan, S. Dildick, K.M. Ecklund, P.J. Fernández Manteca, S. Freed, P. Gardner, F.J.M. Geurts, A. Kumar, W. Li, O. Miguel Colin, B.P. Padley, R. Redjimi, J. Rotter, E. Yigitbasi, Y. Zhang

University of Rochester, Rochester, New York, USA
A. Bodek, P. de Barbaro, R. Demina, J.L. Dulemba, C. Fallon, A. Garcia-Bellido, O. Hindrichs, A. Khukhunaishvili, P. Parygin[83], E. Popova[83], R. Taus, G.P. Van Onsem

The Rockefeller University, New York, New York, USA
K. Goulianos

Rutgers, The State University of New Jersey, Piscataway, New Jersey, USA
B. Chiarito, J.P. Chou, Y. Gershtein, E. Halkiadakis, A. Hart, M. Heindl, D. Jaroslawski, O. Karacheban[25], I. Laflotte, A. Lath, R. Montalvo, K. Nash, H. Routray, S. Salur, S. Schnetzer, S. Somalwar, R. Stone, S.A. Thayil, S. Thomas, J. Vora, H. Wang

University of Tennessee, Knoxville, Tennessee, USA
H. Acharya, D. Ally, A.G. Delannoy, S. Fiorendi, T. Holmes, N. Karunarathna, L. Lee, E. Nibigira, S. Spanier

Texas A&M University, College Station, Texas, USA
D. Aebi, M. Ahmad, O. Bouhali[94], M. Dalchenko, R. Eusebi, J. Gilmore, T. Huang, T. Kamon[95], H. Kim, S. Luo, S. Malhotra, R. Mueller, D. Overton, D. Rathjens, A. Safonov

Texas Tech University, Lubbock, Texas, USA
N. Akchurin, J. Damgov, V. Hegde, A. Hussain, Y. Kazhykarim, K. Lamichhane, S.W. Lee, A. Mankel, T. Mengke, S. Muthumuni, T. Peltola, I. Volobouev, A. Whitbeck

Vanderbilt University, Nashville, Tennessee, USA
E. Appelt, S. Greene, A. Gurrola, W. Johns, R. Kunnawalkam Elayavalli, A. Melo, F. Romeo, P. Sheldon, S. Tuo, J. Velkovska, J. Viinikainen

University of Virginia, Charlottesville, Virginia, USA
B. Cardwell, B. Cox, J. Hakala, R. Hirosky, A. Ledovskoy, A. Li, C. Neu, C.E. Perez Lara

JHEP03(2024)134

Wayne State University, Detroit, Michigan, USA
P.E. Karchin

University of Wisconsin - Madison, Madison, Wisconsin, USA
A. Aravind, S. Banerjee, K. Black, T. Bose, S. Dasu, I. De Bruyn, P. Everaerts, C. Galloni, H. He, M. Herndon, A. Herve, C.K. Koraka, A. Lanaro, R. Loveless, J. Madhusudanan Sreekala, A. Mallampalli, A. Mohammadi, S. Mondal, G. Parida, D. Pinna, A. Savin, V. Shang, V. Sharma, W.H. Smith, D. Teague, H.F. Tsoi, W. Vetens, A. Warden

Authors affiliated with an institute or an international laboratory covered by a cooperation agreement with CERN
S. Afanasiev, V. Andreev, Yu. Andreev, T. Aushev, M. Azarkin, A. Babaev, A. Belyaev, V. Blinov[96], E. Boos, V. Borshch, D. Budkouski, V. Bunichev, V. Chekhovsky, R. Chistov[96], M. Danilov[96], A. Dermenev, T. Dimova[96], D. Druzhkin[97], M. Dubinin[87], L. Dudko, A. Ershov, G. Gavrilov, V. Gavrilov, S. Gninenko, V. Golovtcov, N. Golubev, I. Golutvin, I. Gorbunov, A. Gribushin, Y. Ivanov, V. Kachanov, L. Kardapoltsev[96], V. Karjavine, A. Karneyeu, V. Kim[96], M. Kirakosyan, D. Kirpichnikov, M. Kirsanov, V. Klyukhin, O. Kodolova[98], D. Konstantinov, V. Korenkov, A. Kozyrev[96], N. Krasnikov, A. Lanev, P. Levchenko[99], N. Lychkovskaya, V. Makarenko, A. Malakhov, V. Matveev[96], V. Murzin, A. Nikitenko[100,98], S. Obraztsov, V. Oreshkin, V. Palichik, V. Perelygin, M. Perfilov, S. Petrushanko, S. Polikarpov[96], V. Popov, O. Radchenko[96], M. Savina, V. Savrin, D. Selivanova, V. Shalaev, S. Shmatov, S. Shulha, Y. Skovpen[96], S. Slabospitskii, V. Smirnov, D. Sosnov, V. Sulimov, E. Tcherniaev, A. Terkulov, O. Teryaev, I. Tlisova, A. Toropin, L. Uvarov, A. Uzunian, A. Vorobyev[†], N. Voytishin, B.S. Yuldashev[101], A. Zarubin, I. Zhizhin, A. Zhokin

[†] *Deceased*
[1] *Also at Yerevan State University, Yerevan, Armenia*
[2] *Also at TU Wien, Vienna, Austria*
[3] *Also at Institute of Basic and Applied Sciences, Faculty of Engineering, Arab Academy for Science, Technology and Maritime Transport, Alexandria, Egypt*
[4] *Also at Ghent University, Ghent, Belgium*
[5] *Also at Universidade Estadual de Campinas, Campinas, Brazil*
[6] *Also at Federal University of Rio Grande do Sul, Porto Alegre, Brazil*
[7] *Also at UFMS, Nova Andradina, Brazil*
[8] *Also at Nanjing Normal University, Nanjing, China*
[9] *Now at The University of Iowa, Iowa City, Iowa, USA*
[10] *Also at University of Chinese Academy of Sciences, Beijing, China*
[11] *Also at University of Chinese Academy of Sciences, Beijing, China*
[12] *Also at an institute or an international laboratory covered by a cooperation agreement with CERN*
[13] *Now at British University in Egypt, Cairo, Egypt*
[14] *Now at Cairo University, Cairo, Egypt*
[15] *Also at Birla Institute of Technology, Mesra, Mesra, India*
[16] *Also at Purdue University, West Lafayette, Indiana, USA*
[17] *Also at Université de Haute Alsace, Mulhouse, France*
[18] *Also at Department of Physics, Tsinghua University, Beijing, China*
[19] *Also at The University of the State of Amazonas, Manaus, Brazil*

JHEP03(2024)134

[20] Also at Erzincan Binali Yildirim University, Erzincan, Turkey
[21] Also at University of Hamburg, Hamburg, Germany
[22] Also at RWTH Aachen University, III. Physikalisches Institut A, Aachen, Germany
[23] Also at Isfahan University of Technology, Isfahan, Iran
[24] Also at Bergische University Wuppertal (BUW), Wuppertal, Germany
[25] Also at Brandenburg University of Technology, Cottbus, Germany
[26] Also at Forschungszentrum Jülich, Juelich, Germany
[27] Also at CERN, European Organization for Nuclear Research, Geneva, Switzerland
[28] Also at Institute of Physics, University of Debrecen, Debrecen, Hungary
[29] Also at Institute of Nuclear Research ATOMKI, Debrecen, Hungary
[30] Now at Universitatea Babes-Bolyai - Facultatea de Fizica, Cluj-Napoca, Romania
[31] Also at Physics Department, Faculty of Science, Assiut University, Assiut, Egypt
[32] Also at HUN-REN Wigner Research Centre for Physics, Budapest, Hungary
[33] Also at Faculty of Informatics, University of Debrecen, Debrecen, Hungary
[34] Also at Punjab Agricultural University, Ludhiana, India
[35] Also at UPES - University of Petroleum and Energy Studies, Dehradun, India
[36] Also at University of Visva-Bharati, Santiniketan, India
[37] Also at University of Hyderabad, Hyderabad, India
[38] Also at Indian Institute of Science (IISc), Bangalore, India
[39] Also at IIT Bhubaneswar, Bhubaneswar, India
[40] Also at Institute of Physics, Bhubaneswar, India
[41] Also at Deutsches Elektronen-Synchrotron, Hamburg, Germany
[42] Also at Department of Physics, Isfahan University of Technology, Isfahan, Iran
[43] Also at Sharif University of Technology, Tehran, Iran
[44] Also at Department of Physics, University of Science and Technology of Mazandaran, Behshahr, Iran
[45] Also at Helwan University, Cairo, Egypt
[46] Also at Italian National Agency for New Technologies, Energy and Sustainable Economic Development, Bologna, Italy
[47] Also at Centro Siciliano di Fisica Nucleare e di Struttura Della Materia, Catania, Italy
[48] Also at Università degli Studi Guglielmo Marconi, Roma, Italy
[49] Also at Scuola Superiore Meridionale, Università di Napoli 'Federico II', Napoli, Italy
[50] Also at Fermi National Accelerator Laboratory, Batavia, Illinois, USA
[51] Also at Università di Napoli 'Federico II', Napoli, Italy
[52] Also at Ain Shams University, Cairo, Egypt
[53] Also at Consiglio Nazionale delle Ricerche - Istituto Officina dei Materiali, Perugia, Italy
[54] Also at Riga Technical University, Riga, Latvia
[55] Also at Department of Applied Physics, Faculty of Science and Technology, Universiti Kebangsaan Malaysia, Bangi, Malaysia
[56] Also at Consejo Nacional de Ciencia y Tecnología, Mexico City, Mexico
[57] Also at Trincomalee Campus, Eastern University, Sri Lanka, Nilaveli, Sri Lanka
[58] Also at Saegis Campus, Nugegoda, Sri Lanka
[59] Also at INFN Sezione di Pavia, Università di Pavia, Pavia, Italy
[60] Also at National and Kapodistrian University of Athens, Athens, Greece
[61] Also at Ecole Polytechnique Fédérale Lausanne, Lausanne, Switzerland
[62] Also at University of Vienna Faculty of Computer Science, Vienna, Austria
[63] Also at Universität Zürich, Zurich, Switzerland
[64] Also at Stefan Meyer Institute for Subatomic Physics, Vienna, Austria
[65] Also at Laboratoire d'Annecy-le-Vieux de Physique des Particules, IN2P3-CNRS, Annecy-le-Vieux, France
[66] Also at Near East University, Research Center of Experimental Health Science, Mersin, Turkey
[67] Also at Konya Technical University, Konya, Turkey
[68] Also at Izmir Bakircay University, Izmir, Turkey
[69] Also at Adiyaman University, Adiyaman, Turkey
[70] Also at Necmettin Erbakan University, Konya, Turkey

JHEP03(2024)134

[71] *Also at Bozok Universitetesi Rektörlügü, Yozgat, Turkey*
[72] *Also at Marmara University, Istanbul, Turkey*
[73] *Also at Milli Savunma University, Istanbul, Turkey*
[74] *Also at Kafkas University, Kars, Turkey*
[75] *Also at Hacettepe University, Ankara, Turkey*
[76] *Also at Istanbul University - Cerrahpasa, Faculty of Engineering, Istanbul, Turkey*
[77] *Also at Yildiz Technical University, Istanbul, Turkey*
[78] *Also at Vrije Universiteit Brussel, Brussel, Belgium*
[79] *Also at School of Physics and Astronomy, University of Southampton, Southampton, United Kingdom*
[80] *Also at University of Bristol, Bristol, United Kingdom*
[81] *Also at IPPP Durham University, Durham, United Kingdom*
[82] *Also at Monash University, Faculty of Science, Clayton, Australia*
[83] *Now at an institute or an international laboratory covered by a cooperation agreement with CERN*
[84] *Also at Università di Torino, Torino, Italy*
[85] *Also at Bethel University, St. Paul, Minnesota, USA*
[86] *Also at Karamanoğlu Mehmetbey University, Karaman, Turkey*
[87] *Also at California Institute of Technology, Pasadena, California, USA*
[88] *Also at United States Naval Academy, Annapolis, Maryland, USA*
[89] *Also at Bingol University, Bingol, Turkey*
[90] *Also at Georgian Technical University, Tbilisi, Georgia*
[91] *Also at Sinop University, Sinop, Turkey*
[92] *Also at Erciyes University, Kayseri, Turkey*
[93] *Also at Horia Hulubei National Institute of Physics and Nuclear Engineering (IFIN-HH), Bucharest, Romania*
[94] *Also at Texas A&M University at Qatar, Doha, Qatar*
[95] *Also at Kyungpook National University, Daegu, Korea*
[96] *Also at another institute or international laboratory covered by a cooperation agreement with CERN*
[97] *Also at Universiteit Antwerpen, Antwerpen, Belgium*
[98] *Also at Yerevan Physics Institute, Yerevan, Armenia*
[99] *Also at Northeastern University, Boston, Massachusetts, USA*
[100] *Also at Imperial College, London, United Kingdom*
[101] *Also at Institute of Nuclear Physics of the Uzbekistan Academy of Sciences, Tashkent, Uzbekistan*